

Alma Mater Studiorum Università di Bologna  
Archivio istituzionale della ricerca

Cognitive approaches to enhance spectrum availability for satellite systems

This is the final peer-reviewed author's accepted manuscript (postprint) of the following publication:

*Published Version:*

Chatzinotas, S., Evans, B., Guidotti, A., Icolari, V.R., Lagunas, E., Maleki, S., et al. (2017). Cognitive approaches to enhance spectrum availability for satellite systems. INTERNATIONAL JOURNAL OF SATELLITE COMMUNICATIONS AND NETWORKING, 35(5), 407-442 [10.1002/sat.1197].

*Availability:*

This version is available at: <https://hdl.handle.net/11585/566746> since: 2022-03-07

*Published:*

DOI: <http://doi.org/10.1002/sat.1197>

*Terms of use:*

Some rights reserved. The terms and conditions for the reuse of this version of the manuscript are specified in the publishing policy. For all terms of use and more information see the publisher's website.

This item was downloaded from IRIS Università di Bologna (<https://cris.unibo.it/>).  
When citing, please refer to the published version.

(Article begins on next page)

This is the final peer-reviewed accepted manuscript of:

*Chatzinotas, S., Evans, B., Guidotti, A., Icolari, V., Lagunas, E., Maleki, S., Sharma, S. K., Tarchi, D., Thompson, P., and Vanelli-Coralli, A. (2017) **Cognitive approaches to enhance spectrum availability for satellite systems**. Int. J. Satell. Commun. Network., 35: 407– 442*

The final published version is available online at: <https://doi.org/10.1002/sat.1197>

#### Rights / License:

The terms and conditions for the reuse of this version of the manuscript are specified in the publishing policy. For all terms of use and more information see the publisher's website.

*This item was downloaded from IRIS Università di Bologna (<https://cris.unibo.it/>)*

***When citing, please refer to the published version.***

# Cognitive Approaches to Enhance Spectrum Availability for Satellite Systems

S. Chatzinotas<sup>1</sup>, B. Evans<sup>2</sup>, A. Guidotti<sup>3</sup>, V. Icolari<sup>3</sup>, E. Lagunas<sup>1</sup>, S. Maleki<sup>1</sup>,  
S.K. Sharma<sup>1</sup>, D. Tarchi<sup>3\*</sup>, P. Thompson<sup>2</sup> and A. Vanelli Coralli<sup>3</sup>

<sup>1</sup> *Interdisciplinary Centre for Security, Reliability and Trust (SnT), University of Luxembourg, L-2721 Luxembourg*

<sup>2</sup> *University of Surrey, United Kingdom*

<sup>3</sup> *Department of Electrical, Electronic and Information Engineering, University of Bologna, 40136 Bologna, Italy*

## SUMMARY

Cognitive Radio technologies have achieved in the recent years an increasing interest for the possible gain in terms of spectrum usage with respect to unshared approaches. While most of the attention has been devoted to the cognitive coexistence between terrestrial systems, the coexistence between terrestrial and satellite communications is also seen as a viable option. CoRaSat (COgnitive RADio for SATellite Communications) has been an European Commission 7th Framework Programme project funded under the ICT Call 8. CoRaSat aimed at investigating, developing, and demonstrating cognitive radio techniques in satellite communication systems for flexible and dynamic spectrum access. In this paper the CoRaSat cognitive approaches and techniques, investigated, developed, and demonstrated as most relevant to Satellite Communications, are described. In particular the focus is on spectrum awareness, i.e., database and spectrum sensing approaches, and on spectrum exploitation algorithms, i.e., resource allocation and beamforming algorithms, to enable the use of spectrum for satellite communications using shared bands.

Copyright © 2016 John Wiley & Sons, Ltd.

Received ...

**KEY WORDS:** Cognitive Radio; Satellite Communications; Spectrum Sharing; Database; Spectrum Sensing; Resource Allocation; ESOMP

## 1. INTRODUCTION

Satellite Communications (SatCom) is a key technology in achieving the challenging objective set forth in the Digital Agenda for Europe to provide high-speed broadband access to everyone by 2020 [1]. The CoRaSat (COgnitive RADio for SATellite communications) project envisaged a flexible and smart satellite system able to exploit unused or underused frequency resources shared

---

\*Correspondence to: Department of Electrical, Electronic and Information Engineering, University of Bologna, 40136 Bologna, Italy. E-mail: daniele.tarchi@unibo.it

Contract/grant sponsor: EU FP7 project CoRaSat (FP7 ICT STREP); contract/grant number: 316779

Copyright © 2016 John Wiley & Sons, Ltd.

Prepared using *satauth.cls* [Version: 2010/05/13 v2.00]

with other services on a primary or secondary basis [2, 3]. The objective was to maximize resource utilization and to open up novel business perspectives with lower transmission costs for which Cognitive Radio (CR) techniques are considered the most promising solution [4].

In this paper, an overview of the most important spectrum awareness and exploitation techniques developed in the context of CoRaSat is presented. First of all a description of the application scenarios and the background on the enabling techniques, with respect to the SatCom environment are given, then the specific techniques that have been developed are discussed, by focusing on both the theoretical analysis and on their numerical assessment.

### *1.1. The CoRaSat Project Vision*

For the first time in SatCom research initiatives, CoRaSat has systematically and thoroughly approached the CR concept considering SatCom. CoRaSat has identified scenarios and use cases, focusing on broadband applications as well as considering other services such as interactive broadcasting, narrowband applications, etc., where cognitive approaches can improve spectrum exploitation. Technology enablers for the identified scenarios were developed and demonstrated for specific use cases through analysis, simulation, and testbed implementations. Flexible spectrum usage has potential benefits for SatCom as well as threats; CoRaSat aimed at demonstrating that the benefits outnumber the threats and enables the gains of new business opportunities. This paper addresses some of the results of the project.

### *1.2. Background*

Following a review of SatCom activities which included technical issues, market studies, regulatory impact and economic value, the CoRaSat team focused on the Ka-band spectrum to address the value of cognitive approaches in terms of application to broadband communications since the demand for higher rate and reliable broadband communications is accelerating all over the world. Within Europe, the Digital Agenda sets a target for universal broadband coverage of at least 30 Mbps across the whole of Europe by 2020 and 100 Mbps to at least 50 percent of the households [1].

Fixed connections and cellular networks cannot alone meet this target in the rural and remote areas and also in some black spots across the coverage. In these latter regions, satellite broadband delivery is the only practical answer as satellite will cover the whole territory. Some recent studies of the roll out of broadband have shown that in 2020 up to 50 percent of households in some regions will only have satellite available as a means of accessing broadband and thus 5-10 million households are potential satellite customers [5]. Current Ku-band satellites do not have the capacity to deliver such services at a cost per bit that makes a business case and thus, the satellite community has turned to High Throughput Satellites (HTS) operating at Ka-band and above. Examples of early Ka-band HTS dedicated to such services are Eutelsat KaSat [6] and VIASAT-1 [7]. These satellites employ multiple (around 100) beams using fourfold frequency reuse over the coverage area to achieve capacity of the order of 100 Gbps per satellite. The latter is limited by the exclusive spectrum available to satellite of 500 MHz in both the up and downlinks and this limits the feasible user rates to 10-20 Mbps. Thus, looking ahead to the increased user demands, we have to look to larger satellites (maybe up to Terabit/s [8, 9]) and to more spectrum. With respect to the Q/V bands,

while they have already been suggested for feeder links, their usage for the user terminals requires additional expense, limiting our analysis to the problem of getting more usable spectrum at Ka band.

The Ka-band exclusive bands for satellite are 19.7 to 20.2 GHz in the downlink and 29.5 to 30 GHz on the uplink. In these bands Fixed Satellite Service (FSS) terminals can operate in an uncoordinated manner, which means that they do not have to apply for and be granted a license by the national regulators, provided they meet target performance characteristics. The issue in other parts of the Ka-band is that the spectrum is allocated, not just to FSS but also to the Fixed Service (FS) and to the uplink of the Broadcast Satellite Service (BSS) as well as Mobile Services (MS).

The International Telecommunications Union (ITU) has allocated this spectrum in the three regions of the world, as shown in Table I for Ka-band (Europe is Region 1). In the so called shared bands, the different services need to co-exist and this is usually done by the process of coordination. For example, a larger gateway or feeder link may use this band but is coordinated and then licensed to operate and receive protection from interference caused by other service users. Within Europe, the European Conference of Postal and Telecommunications Administrations (CEPT - Conférence Européenne des administrations des Postes et des Télécommunications) [10] has adopted decisions that expand those of the ITU and produce tighter regulation as follows:

- 17.3-17.7 GHz: BSS feeder links are considered as the incumbent links but uncoordinated FSS links are also permitted.
- 17.7-19.7 GHz: FS links are considered incumbent but FSS terminals may be deployed anywhere but without right of protection.
- 27.5-29.5 GHz: CEPT provides a segmentation of the band between FSS and FS portions as shown in Figure 1. Within each segment there is a specified incumbent, even if FSS terminals can operate in FS portions provided they do not interfere with the incumbent FS.

Table I. Extract of ITU Frequency Allocations.

Frequency bands	ITU Region 1	ITU Region 2	ITU Region 3
17.3-17.7 GHz (Scenario A)	FSS (space-Earth) BSS (feeder links) Radiolocation	FSS (space-Earth) BSS (feeder links) Radiolocation	FSS (space-Earth) BSS (feeder links) Radiolocation
17.7-19.7 GHz (Scenario B)	FSS (space-Earth) BSS (feeder links @18.1 GHz) FS	FSS (space-Earth)  FS	FSS (space-Earth) BSS (feeder links @18.1 GHz) FS
27.5-29.5 GHz (Scenario C)	FSS (space-Earth) FS MS	FSS (space-Earth) FS MS	FSS (space-Earth) FS MS

The work reported in this paper has been conducted within the EU FP7 project CoRaSat [3, 2, 11, 12] that examines different possibilities in which FSS satellite terminals in the Ka-band can co-exist with FS and BSS links given the regulatory regime presented above. In particular the focus is on the assessment of some specific spectrum awareness and exploitation techniques for selected scenarios. After a careful revision of the proposed classes of techniques, also with respect to the literature, the proposed algorithms are described by giving also some numerical results for evaluating their effectiveness.

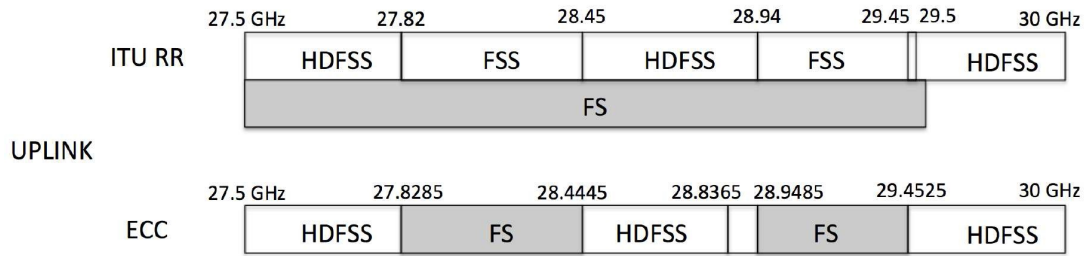


Figure 1. European Spectrum allocation.

The paper is organized as follows: in Section 2, the scenarios proposed in the CoRaSat project and the system model are described. In Section 3, the proposed approaches for the spectrum awareness and exploitation are described, while in Section 4, the analysis of the numerical results is given. Finally, in Section 5, some conclusions are drawn.

## 2. SCENARIO AND SYSTEM MODEL

### 2.1. Scenarios

Within the CoRaSat project, three Ka-band scenarios have been investigated, reflecting the three spectrum components detailed in the previous section. In Figure 2, we illustrate the considered scenarios with the respective interference paths. In the first two scenarios the FSS is supposed to be in downlink: scenario A (17.3-17.7 GHz), where the potential interference is from BSS uplinks, and scenario B (17.7-19.7 GHz), where the potential interference is from incumbent FS transmitters. In both of these cases, the FSS is permitted to operate but is not protected by the regulatory regime and thus it is important to ascertain the level of the interference and its effect on the FSS received signal. The third scenario C works in the transmit band of the FSS from 27.5-29.5 GHz and the interference is from the FSS transmitting earth station into the FS receivers, which are to be protected. The latter is more critical in that we need to demonstrate that the FSS does not contravene interference limits imposed by the regulatory regime.

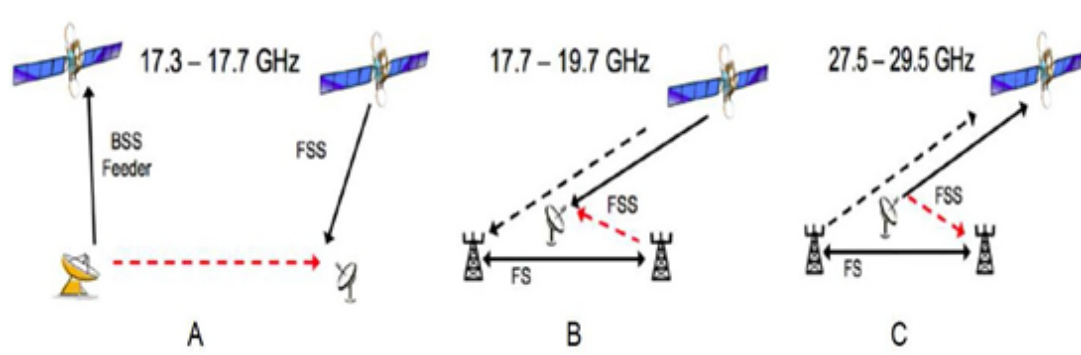


Figure 2. Scenarios in CoRaSat.

## 2.2. Enabling Techniques

In order to cope with the system and regulatory requirements in the selected scenarios, the following enabling techniques have been taken into consideration: Databases and Spectrum sensing for the spectrum awareness phase and Beamforming and Resource allocation for the spectrum exploitation phase.

In particular, such enabling technologies are contrasted against specific technical requirements and, if they satisfy the technical requirements, evaluated on the basis of the produced improvement on several Key Performance Indexes (KPIs). The proposed methodology is shown in Figure 3 [13]. Satellite Manufacturers and Operators produce inputs in terms of the required system input parameters and the QoS targets. This information, combined with ITU Radiocommunication (ITU-R) and Electronic Communications Committee (ECC) regulations, leads the design of spectrum awareness and interference modeling techniques (enabling technologies), which produce an output of spectrum exploitation in terms of spectrum cartographies and noise contour floors. Once this scenario-level analysis is completed, a network management analysis is performed, in particular facing resource allocation and interference management techniques. The last step is the comparison of each of the proposed solutions for each scenarios through properly defined KPIs, which has led the selection of the most promising and feasible approaches.

From the involved entities point of view instead, the databases are taken into account offline, and used for evaluating the interference level in all the interested areas. On the other side instead the spectrum sensing is performed by the interested terminals. Since in the considered scenarios, the cognitive terminal are always those belonging to the satellite links, we consider in the following that the satellite terminals are those involved in the spectrum sensing operations. By resorting to the Figure 3, the network management is performed by the Network Control Center, that has also the role of requesting the results of the spectrum sensing for the terminals when needed (e.g., for absence or incompleteness of the data derived from the databases)

**2.2.1. Databases** The database approach adopts a chosen propagation channel model and employs databases of interfering sources to derive interference levels that can then be used to check if they are capable of being mitigated, if required. Thus, in the chosen scenarios the calculation of interference can be performed if one has obtained the corresponding accurate FS database, which includes the characteristics and locations of the potential interferers, then using this with equipment models, propagation models and the path details. Similar ideas have been employed in Television White Space (TVWS) systems [14] to allow UHF frequencies to be used in the gaps between TV transmission regions.

For scenario A, the number of BSS uplinks in Europe is small and thus a database system is similar in magnitude to that of TVWS. However, for scenarios B and C the number of FS links runs into the tens of thousands and the database is much more complex. The data on the positions and the characteristics of the BSS and FS are generally held by national regulators and these need to be available for a database system to work.

The information from a real interferer database is interfaced to an interference modeling engine, which uses ITU-R Recommendation P.452-15 [15] procedures plus terrain and other databases. This is the latest version of the ITU Recommendation that contains a prediction method for the

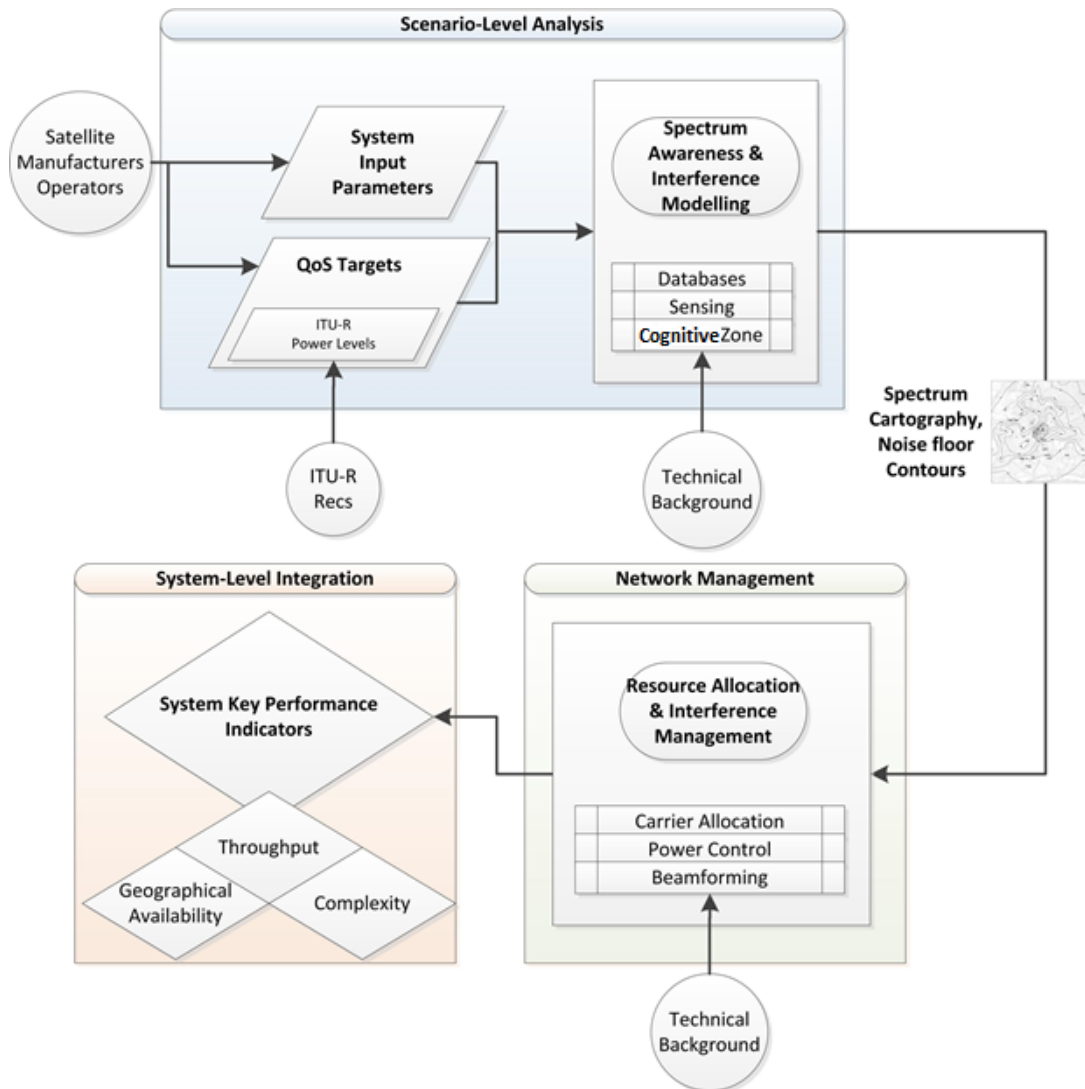


Figure 3. The proposed assessment methodology.

evaluation of path loss between stations. ITU-R P.452-15 includes all the propagation effects on the surface of the Earth at frequencies from 0.1 GHz to 50 GHz. In addition, other factors, which affect interference calculation, such as terrain height and bandwidth overlapping are also considered in the proposed database approach, which is illustrated in Figure 4.

The typical interference threshold we determine is based on the long term interference, which can be expected to be present for at least 20 percent of the average year and it is set at 10 dB below the system noise floor. The interference thresholds for FSS and FS reception are, respectively, -154 dBW/MHz and -146 dBW/MHz, respectively as given in [16, 17]. Having determined the interference level at the FSS (in scenarios A or B) it can be compared with the regulatory threshold. The action is then taken in the resource allocation at the gateway where a new carrier can be assigned either in another part of the *shared band*, where interference is acceptable, or in the exclusive band.

For the scenario C, the databases are, instead, used with a different aim, since the interference is caused by the FSS into the FS. Here the database is used to calculate the maximum permissible



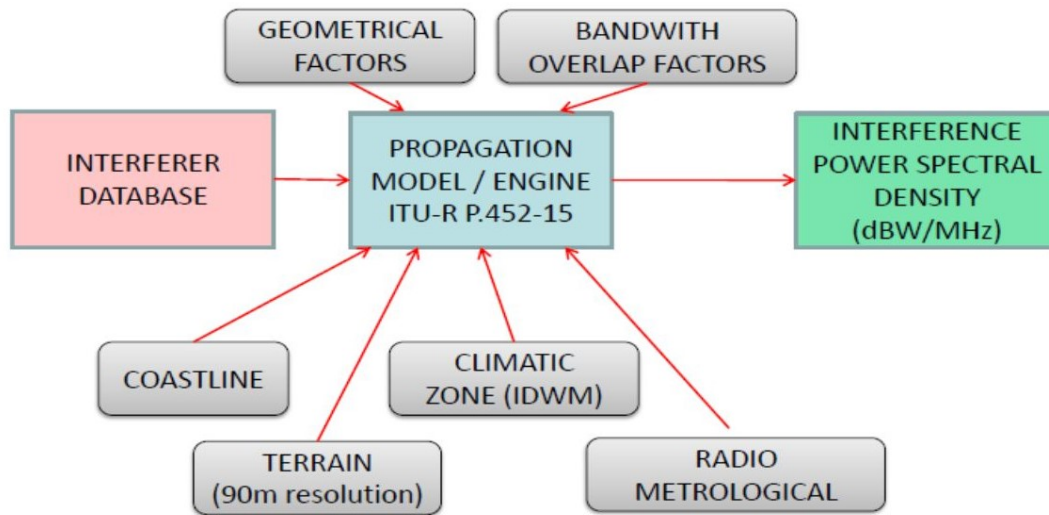


Figure 4. Database Modeling Approach.

power that can be transmitted from the FSS such that the FS links in the vicinity have an interference that remains below the threshold. Further details on the implementation of this enabling technology are presented in Section 3.1.

The data base scheme obviously relies on their availability from the Regulators. A number of the European regulators have now placed them on line and others will follow under pressure from the CEPT. These data bases are accurate as the licensing of the links is governed by them. Data bases can be used to produce interference maps which can be made available to satellite operators to advise on FSS deployments. The maps can be produced either by Regulators, satellite operators or by third parties organised by CEPT. The manufacturers of satellite network gateways can integrate the maps into their resource allocation schemes which will then automate the carrier allocations. Another option in the case where data bases are not available is to use the SINR/spectrum sensing algorithm at the gateway to drive the carrier allocation. The latter could also be used to augment the data base scheme.

**2.2.2. Spectrum Sensing** Even if databases can give much of the needed information for coping with the spectrum awareness in a given area, cognitive techniques cannot rely only on databases. Spectrum sensing techniques should be used as well. In fact, spectrum sensing techniques can complement the databases information in case of fast changes in the environment and if database is not available or is too old for a given area. The aim of spectrum sensing is the detection of the signals belonging to other communication system by scanning selected frequency bands, which is useful to understand the usage of a certain spectrum portion.

The parameters which mainly affect the performance of a general spectrum sensing technique, and thus the cognitive radio system, are:

- 1 *Sensing periodicity*: Sensing periodicity determines the period where the probability of the incumbent user returning to a specific band is almost zero,

- 2 *Detection technique and complexity*: specific determination of the detection technique depends on the level of the prior knowledge as well as the acceptable complexity of the technique,
- 3 *Probability of false alarm and detection*: probability of false alarm and detection are two fundamental KPIs of any detection technique. A high probability of false alarm corresponds to wrongly detect the presence of an incumbent user, leading to an under-utilization of the unused resources, while a low probability of detection corresponds to not detecting the presence of an incumbent user, leading to transmission wastage and unwanted interference. The minimum value of the probability of detection and maximum value of the false alarm depends on the minimum QoS,
- 4 *Bandwidth*: Spectrum sensing is often performed over a wide-band of frequencies. The same holds for satellite scenarios.

With respect to spectrum sensing for cognitive radio systems, several techniques are proposed and investigated in the literature [18, 19, 20]. Three of the most common techniques which are considered are energy detection [21], cyclostationary feature detection [22] and matched filtering [23].

However, the satellite environment behaves in a different way with respect to classical terrestrial cognitive scenarios. Indeed, a shared terrestrial-satellite environment is characterized by a very high power imbalance between the satellite and the terrestrial links due to the very different link length between the two systems. This evidence changes somehow the approach that should be used when the spectrum awareness should be employed. Indeed, even if we are still interested in having knowledge of the primary system like in a classical cognitive radio system, in the scenarios A and B, the incumbent link is the FS link, while at the same time the cognitive link, represented by the satellite link, cannot interfere the incumbent link. This means that, on the contrary with respect to a classical cognitive radio scenario, now we are much more interested in understanding if in a given area a certain cognitive satellite link can be implemented and can respect some given requirements, given the possible interference generated by a pre-existing FS link. In the scenario C, instead, spectrum sensing cannot be used at the satellite terminal side since no inference occur from the terrestrial to the satellite link.

To this aim a novel approach, where the detection of the incumbent signal is performed jointly with the estimation of its power level, is proposed to be used. This approach allows to have a soft detection of the incumbent presence that allows to exploit in a more efficient way the channel in an underlay fashion.

Moreover, in the considered scenarios, since we have knowledge of the interference level produced by the incumbent against the cognitive, such an approach is more practical in terms of spectrum awareness. Thus, we extend the concept of spectrum sensing through the energy detection with that of SINR estimation. This increased degree of awareness allows the cognitive system to exploit flexibly the available bands whether a spectrum hole is identified or the presence of an incumbent.

As it will be detailed in the Section 3.2, the estimation process is performed through the SNORE algorithm [24, 25] and it is performed in a DA (Data Aided) operating mode (DA-SNORE) [26].

**2.2.3. Beamforming** A widely recognized approach to enhance the cognitive system's performance is to exploit spatial diversity by using multiple antennas. Adaptive antenna arrays represent a promising solution for the radio interference problem since they give the possibility to control the radiation pattern in an adaptive way. In particular, one use of multiple antennas consists in electronically steering the main beam to a given direction while restricting the radiation into certain angular directions. In doing so, the cognitive opportunities will increase. In the context of a terrestrial CR, the concept of null interference constraints has been widely investigated [27, 28]. However, in the context of cognitive satellite communications, only a few papers exist in the literature [29, 30].

In [29], authors have proposed sector-based transmit beamforming at the terrestrial base station considering the spectral coexistence of satellite and terrestrial networks operating in the C band (3.7-4.2 GHz) with the FSS forward link as the primary and the terrestrial downlink as the secondary. In the similar context, in [30], authors have proposed sector-based receive beamforming at the terrestrial base station by utilizing the specific characteristic of the geostationary FSS terminals that they always point towards the GEO satellites and interference observed at the terrestrial base station is concentrated in a specific sector. Whereas, in the current work, we propose to employ receive beamforming techniques at the FSS terminals operating in the Ka-band downlink in order to mitigate harmful interference coming from terrestrial FS transmitters.

For the considered scenarios, beamforming techniques can be implemented either at the FSS terminal or at the satellite. Transmit (scenario C) or receive (scenarios A and B) beamforming techniques can be applied at FSS terminal in order to mitigate interference towards the incumbent terminals or to avoid interference coming from the incumbent transmitters. For scenarios A and B, transmit beamforming can be used at the satellite in order to improve the Signal-to-Interference plus Noise Ratio (SINR) at the FSS terminals. In Scenario C, the satellite can apply beamforming in order to maximize the SINR of the worst case users. However, beamforming at the satellite needs additional processing algorithms at the gateway and is more suited to the future generation of multibeam satellites. Therefore, in this paper, we review the FSS terminal beamforming techniques proposed in the context of CoRaSat project for scenarios A and B. Beamforming for scenario C is not considered in this paper. This is because of the capabilities of the return link to control the transmit power and bandwidth, which we prove to be a good mechanism to control the created interference. For detailed description of the receive beamforming techniques reviewed in this paper, readers may refer to [31, 32, 33]. Clearly, a major upgrade in the terminal side is needed since a terminal equipped with multiple antennas is required to design the appropriate radiation pattern. The number of antennas is limited to 2-3 due to cost, mechanical support and electromagnetic blockage issues [34]. Moreover, beamforming at the terminal can only be used to create nulls towards BSS/FS directions if prior information about their locations is known beforehand. In the considered scenarios, the location of BSS/FS stations can be obtained from the database. The beamforming technique adopted in this paper is described in detail in Section 3.4.

**2.2.4. Resource Allocation** Once the available cognitive resources are determined, they need to be allocated to the cognitive users by the network management unit. Resource allocation for terrestrial CR has been studied in detail in different settings [35, 36, 37]. Only a few works have examined Radio Resource Management (RRM) strategies under the cognitive satellite communications

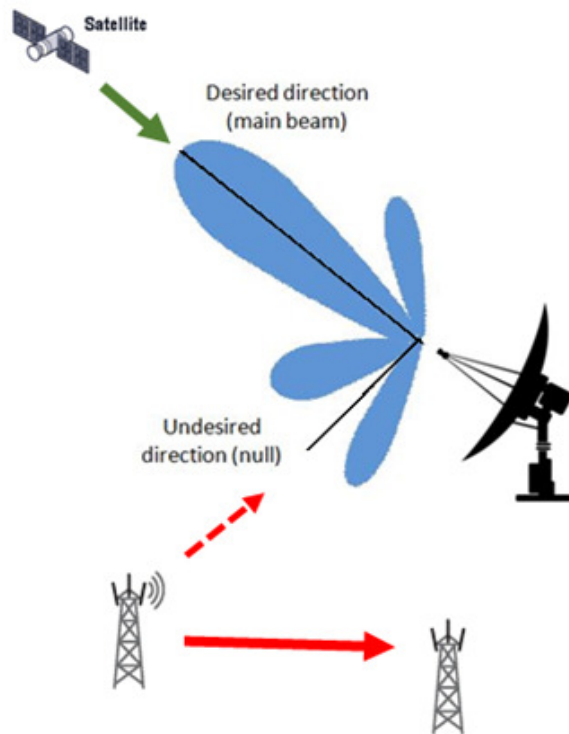


Figure 5. Beamforming at the FSS terminal in scenario B.

framework [38]. Smart resource allocation can be applied to alleviate the interference thereby increasing the spectrum sharing opportunities. Resource allocation techniques should be adapted to each scenario. Clearly, RRM techniques would be different for the downlink satellite transmission compared with the uplink counterpart. Therefore, we distinguish between RRM for scenarios A and B (downlink) and RRM for scenario C (uplink).

In this paper, we are particularly interested in allocating the carrier frequencies available at the satellite system including both shared and exclusive carriers. Moreover, we consider transmit power and bandwidth allocation together with carrier allocation for scenario C. The resource management is carried out at the Network Control Center (NCC) of the satellite system. Essentially, in the downlink, the carrier frequencies are optimally assigned within the satellite transponder to maximize the sum-rate of the satellite system according to their interference conditions. In the uplink scenario, on the other hand, the transmitted power and the bandwidth come into play. While it is not reasonable to assume a power and bandwidth control algorithm at the in-orbit satellite, the transmitter power and the bandwidth of the FSS terminals can be controlled. To comply with regulations, the uplink power density of the FSS system has to ensure that the interference impact on the potentially present FS links does not exceed certain interference limitations. Therefore, in order to satisfy the interference constraint, transmitted powers, bandwidths and carrier frequencies should be considered jointly, since they are key factors in the total interference seen from the incumbent receivers. Both downlink and uplink assume the availability of a database. In particular, a database is needed in the downlink scenarios to estimate the interference received at the FSS terminal. Similarly, a database is needed in the uplink scenario to determine the interference caused at the

incumbent system. If only a partial or no database is available, then spectrum sensing techniques can be considered to enable the application of the proposed techniques.

### 3. PROPOSED APPROACHES

As introduced in 2.2, the CoRaSat approach behaves on the joint utilization of different techniques enabling both awareness and exploitation of the terrestrial links underused spectral resources by the satellite links. The approach adopted is to first use a *spectrum awareness* technique - either database or spectrum sensing. Then having assessed the interference to use *interference mitigation*, e.g., resource allocation at the satellite gateway to allocate carriers such as to avoid unacceptable interference. In the rare occasions that this cannot be done in the shared or exclusive bands then beamforming would be an appropriate mitigation.

#### 3.1. Database and Interference modeling

The Database approach described earlier requires a range of additional data to augment the FS database such that the appropriate model gives an accurate result. Key parameters of the chosen Ka-band VSAT terminal are in Tables II and III.

Table II. VSAT Terminal transmission parameters.

Antenna size	0.77x0.72 m
antenna gain	45.5 dBi
Max TX power	3 W
eirp	48.4 dBW
pointing loss	0.30 dB

Table III. VSAT Terminal receiving parameters.

Antenna size	0.77x0.72 m
antenna gain	42.1 dBi
Noise Figure	2.0 dB
LNA Noise temp	170 K
Antenna noise temperature	78 K
pointing loss	0.30 dBi
Total system noise temp	262 K
nominal G/T	17.3 dB/K
Antenna Radiation Pattern	(ITU-R) REC S.465-6 [39]

In the following some specific FSS GSO locations were adopted for the analysis, resulting in a reasonable range of practicable elevation angles. Such longitudinal orbit locations are: 53E, 13E, 0E and 34W.

Interference calculations were based upon results expressed in terms of spectral density in units of dBW/MHz as this is smaller than the minimum bandwidth in the FS and FSS systems. The analysis

was conducted for long term interference (generally 20%), by assuming that Adaptive Coding and Modulation (ACM) will mitigate short duration interference events including rain fades.

The modeling approach adopted requires a number of physical and radio-meteorological parameters for use with the modeling tool:

- Climatological parameters;
- Radio Climatic Zone Type;
- Terrain Height Data;
- Coastline Database.

**Climatological parameters** The ITU-R P.452 [15] path propagation model requires two climatological parameters:

1. The average sea level value of surface refractivity,  $N_0$  (expressed in 'N-units').
2. The average annual value of  $\Delta N$ , the difference in the values of the refractivity at the surface and 1000m above the surface, (expressed in 'N-units/Km').

These are required for the diffraction and troposcatter sub-models respectively. Digital maps of median annual  $\Delta N$  and median annual  $N_0$  have been prepared and made available on the ITU-R/SG3 website [40]. These new digital maps have been derived from a new analysis of a ten-year (1983 to 1992) global dataset of radiosonde ascents.

**Radio Climatic Zone Type.** Some of the propagation elements of the model in ITU-R P.452 [15] require knowledge of the Radio Climatic Zones as detailed below. The chosen source for obtaining the Radio Climatic Zone at a given latitude and longitude is the ITU Digitised World Map (IDWM) and associated Subroutine Library. This package can be purchased from the ITU [41]. The employed radio-climatic zones are:

- **A1 Coastal:** Land and shore areas, i.e., land adjacent to the sea up to an altitude of 100 m relative to mean sea or water level, but limited to a distance of 50 km from the nearest sea area. Where precise 100 m data are not available, an approximate value, i.e. 300 ft, may be used.
- **A2 Inland:** All land, other than coastal and shore areas defined as coastal land above.
- **B Sea:** Seas, oceans and other large bodies of water (i.e. covering a circle of at least 100 km in diameter)

**Terrain Height Data.** The NASA Shuttle Radar Topographic Mission (SRTM) has provided a Digital Elevation Model (DEM) for over 80% of the globe. The SRTM digital elevation data, produced by NASA, originally provided accurate digital mapping of the world. The SRTM digital elevation data provided by the CGIAR-CSI GeoPortal [42] has been processed to fill data voids, and to facilitate ease of use by a wide group of potential users for the entire world. The data files obtained online were translated to binary format to facilitate fast access to the specific data. It is important to understand that the data in the SRTM 90m datasets is only notionally having a resolution of 90 m and is really a 3-arc-second product where the values in the files are in increments of latitude of 3 arc seconds (0.000833333 degrees). The data is related to the WGS84 reference ellipsoid [43].

The rather large database is broken down into various tiles. For the UK, we use nine tiles (each of approximately 180 MB), translated to binary format. The tiles are 5 degree by 5 degree in size.

**Coastline Database.** For the creation of the coastline in the model, the Global Self-consistent, Hierarchical, High resolution Geography (GSHHG) Database from the US National Oceanic and Atmospheric Administration (NOAA) National Geophysical Data Center [44] is used.

*3.1.1. Bandwidth considerations* There is a need to consider the bandwidths of the interferer and the victim carriers. In the event that the two bandwidths are similar (as in Scenario A), the situation is relatively easy to handle.

In general two situations exist. The first is when a wideband signal is interfering with a narrow band signal and the second is vice versa. For the first case, the impact of the interferer can be readily managed by considering the portion of the interfering signal spectral density within the receiver modem filter bandwidth. Such an approach has sound technical background. It is sufficient for our purposes to consider the receiver modem filter to be a brick wall filter with its bandwidth equal to the stated RF bandwidth.

For the second case, there are no known theoretical models to apply as the performance of the internal elements of the demodulator (such as bit timing and carrier recovery features) have significant roles to play. A simplistic empirical model is often employed where the interfering power is spread over the victims receiver bandwidth. Laboratory measurements that support the above model give confidence in the approach.

If more than one interfering carriers in the victims receiving bandwidth is present, they all need to be assessed and the interfering powers summed. The Appendix 1 of Annex 3 of the Recommendation ITU-R S.740 [45] relates to some of the discussion above and can provide further insight.

### *3.2. Joint Spectrum Estimation and Detection*

As anticipated in the Section 2, the database approach should be complemented by introducing a spectrum sensing algorithm. Moreover, we have also highlighted that a classical spectrum sensing approach could be a limitation in the considered scenario due to the power unbalance between the incumbent and cognitive links. To this aim we resorted to a joint estimation and detection technique that, based on the SNORE algorithm, allows to not just detect but also estimate the incumbent power level in order to assess the feasibility of using a cognitive transmission.

The block diagram of the SNORE algorithm is reported in Fig. 6. While the interested reader could refer to [24, 25], it is worth to notice the the algorithm is based on a comparison between the average received signal and the average of the signal without the data dependency, so as to estimate the SINR at the receiver side.

It is worth to be noticed that the proposed technique based on the DA-SNORE algorithm exploits the cognitive communication links structure for estimating the interference level; this means that it can be used for both Scenarios A and B without major modifications.



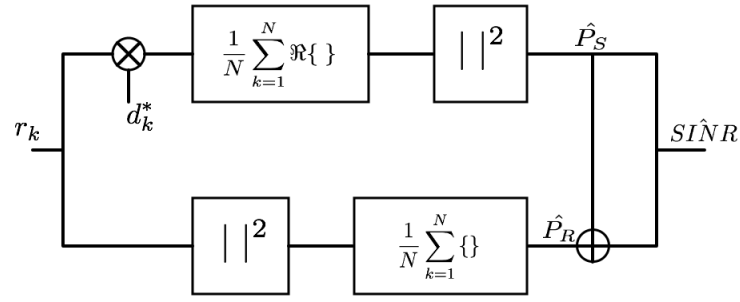


Figure 6. SNORE block diagram

**Technique Design** We assume that the receiver earth terminals are equipped with a receiving chain able to scan all the frequencies of interest with a sensing sub-band,  $B_W$ , equal to 36 MHz, which is the typical bandwidth of DVB-S2 and DVB-S2X [46, 47] communications. Thus, the available non exclusive spectrum is split into  $K$  sub-bands, and for each of these bands the DA-SNORE algorithm [24, 25] is used in order to assess whether incumbent activities are present or not. The incumbent signal operates using different bandwidths but, since we are interested in finding bandwidths in which the cognitive transmission can be established, we can consider as sensing bandwidth 36 MHz and perform estimation in each carrier sequentially.

Since the Data Aided operating mode needs to receive data from the cognitive system in order to estimate SINR, we assume that the earth terminal antenna pointing at the satellite performs the estimation. The choice to estimate by means of the terminals antenna is also favorable since the estimated interference without increasing complexity is exactly the one that affects data reception. In case of perfect synchronization, the Data Aided estimation algorithm can be performed by means of a stream of known symbols that in the case of DVB-S2 or DVB-S2X can be either pilot blocks included in the physical frame or dummy frames sent to the earth terminal here used for the specific purpose of estimation. Further information on DVB-S2X structure are not reported due to space constraints, but they can be obtained in [47, 48].

Assuming that the estimation is performed by means of the pilot blocks regularly inserted within the frame structure of the standard, for each of the  $K$  sub-bands, the time required to estimate the SINR depends on the number of pilot blocks  $W$  required for the estimation process. The choice of  $W$  is based on the target estimation accuracy. Thus, a detailed analysis of the design technique and its parameters is fundamental in order to provide to the cognitive system a timely but affordable knowledge about spectrum activities.

The SINR between the useful received signal power  $P_0$  and the interference plus noise power  $N_0 + \sum_k^{N_i} P_k$ , can be estimated as [24, eq. (2)]:

$$\widehat{SINR} = \frac{\hat{P}_0}{\hat{P}_R - \hat{P}_0} \quad (1)$$



where

$$\begin{aligned}\hat{P}_0 &= \left[ \frac{1}{WN_s} \sum_{l=1}^W \sum_{m=1-lN_{slot}}^{N_s-lN_{slot}} r(m) s_P(|m|_{N_{slot}}) \right]^2 \\ \hat{P}_R &= \frac{1}{WN_s} \sum_{l=1}^W \sum_{m=1-lN_{slot}}^{N_s-lN_{slot}} |r(m)|^2\end{aligned}\quad (2)$$

are, respectively, the estimated useful power and the total estimated received power.

In (2)  $r(t)$  is the the lowpass equivalent expression of the signal at the cognitive receiver,  $W$  represents the number of pilot blocks used during the SNORE estimation,  $N_s$  is the number of pilots in each pilot block,  $N_{slot}$  denotes the slot block length (also equal to the distance between two pilot blocks) and  $s_P(|m|_{N_{slot}})$  represents the  $m$ -th complex symbol belonging to a certain pilot block. The operator  $|\cdot|_{N_{slot}}$  is the modulo- $N$  operator with length  $N_{slot}$ .

It is worthwhile highlighting that the estimation performance strongly depends on  $W$ , as the more pilots blocks are accumulated, the lower the estimation error will be. On the other hand, increasing the number of pilot blocks to be accumulated also requires longer sensing periods. Hence, in order to provide a reliable estimation, an upper and a lower bound can be defined for  $W$ . Thus, starting from the shown results, by exploiting the methodology introduced in [24], the explicit expressions highlighting the relationships between  $W$ , SINR, the estimation error variance  $\sigma_\epsilon^2$ , and the Cramer-Rao bound (CRB) for the design of the proposed cognitive technique are derived. It is possible to derive the closed-form expression of the number of pilot blocks  $W$ :

$$W = \frac{1}{N_s} \left( \frac{3}{2} + \frac{SINR^2}{CRB} \left( \frac{2}{SINR} + 1 \right) \left( \frac{1}{2} + \sqrt{1 + \frac{6CRB}{SINR(2 + SINR)}} \right) \right) \quad (3)$$

as a function of the Cramer-Rao bound, the SINR, and the number of pilots per block  $N_s$ . The number of pilot blocks required to achieve a target error variance  $\sigma_\epsilon^2|_t$  as a function of the SINR can be instead evaluated by solving the third degree equation:

$$W^3 N_s^3 - \left( \frac{11}{2} + \frac{SINR}{\sigma_\epsilon^2} (SINR + 2) \right) W^2 N_s^2 + \left( \frac{39}{4} - \frac{1}{2\sigma_\epsilon^2} + 2 \frac{SINR}{\sigma_\epsilon^2} \right) W N_s - \frac{45\sigma_\epsilon^2 - 4}{8\sigma_\epsilon^2} = 0 \quad (4)$$

In order to give a reliable and timely estimation on the interference, the scanning operation is usually performed periodically. According to the derived equation is therefore possible to define and optimize this periodicity. In particular, a first more accurate evaluation of the presence of incumbents' interference can be performed over the frequency range when no data transmission is required. This operation is denoted as the *initial sensing phase*. When a transmission is established in a non exclusive band, the potential interference caused by a incumbent should then be periodically estimated by the user in that specific band, in order to control if the target QoS for the cognitive system can still be guaranteed. This operation is denoted as the *fast in-band sensing*, and it is performed during data transmission. With this approach, it is possible to sense with a very low duty

cycle, in order to guarantee the desired capacity and satisfy QoS requirements without increasing the computational load on the cognitive system.

Besides discussion on the periodicity with which the sensing task is performed, also distinction on its operating point are needed. Different interference sources, which the cognitive system has to cope with, are foreseen. The interference in the cognitive earth terminal might come from a secondary lobe that generates a lower interference than the interference from a highly directive FS incumbent link. As a consequence, the number of pilot blocks for estimation has also to be designed according to the interference levels that the cognitive terminal will experience and the targeted estimation errors [26].

**Technique Adaptation** Even if the proposed SNORE based interference estimation algorithm is a promising approach, a proper calibration and adaptation of the cognitive scenarios under realistic impairments is needed. The overall expected link performance is assumed known from planning and previous link budget exercises before installation. This results in an expected signal to noise ratio to be met during the correct functioning of the terminal. However, a difference from the expected SNIR may result from perturbations or inaccuracies in the overall system that needs to be addressed with the NCC integration of the spectrum sensing techniques. The typical impairments that can occur during the common functioning of the system, are:

- Rainfade and atmospheric attenuation during terminal installation
- Inaccurate antenna pointing of the terminal
- Cross polarization interference
- Bias in expected SNIR value resulting from margins at different levels
- Interference from other satellite downlinks or adjacent beams of the same system
- Interference from incumbent users
- Receiver gain variation
- LNB gain variation over temperature

Imperfect alignment of the transmitting and receiving antennas could cause pointing errors that are sources of additional losses. These losses are due to a reduction of the antenna gain with respect to its maximum and are function of the misalignment of the angle of reception. Other losses of earth terminals, which are due to non idealities, are feeder losses  $L_{FRX}$  between the antenna and the receiver, and polarization mismatch losses  $L_{POL}$ . These impairments raises during the terminal installation and they have to be detected and taken into account.

Atmospheric events can cause additional attenuations and variations with respect to the common free space loss propagation. Several effects are present but an overall contribution affecting the received power can be taken into account by adding to the free space loss attenuation  $A_{FS}$ , the contribution  $A_P$  that includes all the atmospheric attenuation:

$$A_{TOT}[dB] = A_{FS}[dB] + A_P[dB].$$

These losses are significant above 10 GHz as in case of the Ka bands, used in the considered scenario. In such bands, tropospheric phenomena are the main contributions of the link availability and service quality degradation. These phenomena are i) attenuation, ii) scintillation, iii)

depolarization and iv) increase of the antenna temperature in the receiving earth terminal. A more detailed description of these phenomena is included in [49, Chapter 3].

In the downlink case, the carrier to noise ratio can be rearranged in order to separate the ideal, or expected value  $\left(\frac{C}{N_0}\right)_{FS}$  calculated in free space loss conditions, from contributions that cause its variation as:

$$\left(\frac{C}{N_0}\right)_{DOWNLINK} [dB] = \left(\frac{C}{N_0}\right)_{FS} - \Delta_1 EIRP_{SAT} - A_p - \Delta_2 \left(\frac{G}{T}\right)_{ES} \quad (5)$$

where  $EIRP_{SAT}$  is the satellite EIRP,  $\left(\frac{G}{T}\right)_{ES}$  the figure of merit of the earth terminal receiver and  $\Delta_1$  and  $\Delta_2$  a possible decrease of the satellite  $EIRP_{SAT}$  and the figure of merit  $\left(\frac{G}{T}\right)_{ES}$ , respectively.  $\Delta_1$  and  $\Delta_2$  includes all the uncertainties considered.

To address all possible sources of practical errors to devise a reliable spectrum sensing technique within the considered cognitive scenarios, a combination of planning tools, reference terminals and a system learning mechanism with feedback and additional mechanisms can be defined. To adapt the spectrum sensing to the practical parameter uncertainty encountered in the system, it is foreseen to enhance the SS-SNIR procedure to include many parameters and make decisions on a multi-parameter basis with an overall tracking of the terminal situation on short and long term.

Based on these parameters, the procedure to identify the potential terrestrial interference event can seen as a task performed at the NCC that continuously monitors these parameters and track them with the aim of estimating the interference level produced by the terrestrial links at each terminal location. Since the overall end-to-end link budget entails different contributions, the main task is to discern the incumbent interference from other sources of perturbation that can impact the end to end link budget. For this purpose, all possible signal trackers for the forward and return link per terminal and their reference and historical data are selected and retained. In Table IV the events and the corresponding impacted parameters are listed.

Table IV. List of event and their impact.

Event / Impact detected	Parameters under observation impacted and impacted elements of network
1./ Interference from incumbent users	SNIR decreases for impacted terminal(s)
2./ Cross polarization interference	SNIR decreases for impacted frequency range on transponder.
3./ Rainfade on downlink at terminal location	SNIR and Received Carrier Power decrease for impacted terminal(s).
4./ Rainfade event on feeder uplink at hub location	SNIR and Received Carrier Power decrease for all terminal(s).
5./ Terminal antenna depointing	SNIR and Received Carrier Power decrease for impacted terminal.
6./ Gain change on the link	Received Carrier Power changes depending on uplink feeder link gain change or terminal (LNB) gain change all or one terminal impacted.

### 3.3. Spectrum Sensing and Database combination

The spectrum sensing techniques can also support and be supported by the use of databases, *i.e.*, a priori known incumbent activities. To this aim we can introduce the cognitive zones [50], defined as the geographical area around an incumbent user station where cognitive radio techniques such as spectrum sensing should be employed to mitigate the interference to an acceptable level. In other words, the interference outside of this area is below the acceptable interference threshold thus, cognitive radio techniques are not necessary. As an example, the cognitive zone refinement and corrections of the considered frequency bands, when the database information is outdated, not fully available or incorrect, can be updated by information provided from the operational terminals. Specific interference signals detected from the incumbent user transmissions can be feedback to the NCC. Especially in large FSS deployed networks and with a certain critical density of the FSS terminals in the vicinity of the incumbent systems, the spectrum sensing technique becomes an important additional option to gain specific interference context knowledge about the interference from incumbent users upon the FSS network. This approach supports the primary database information and complements it and makes the entire system more resilient with respect to potential database errors.

### 3.4. Resource Allocation

This section aims at optimizing the allocation of available resources, while employing interference management techniques such as beamforming or power control. As mentioned before, resource allocation techniques should be adapted to each scenario. In this section, we first describe the resource allocation strategy for the downlink (scenario A and B). Secondly, the uplink (scenario C) is considered.

**3.4.1. Scenario A & B (downlink)** For the cognitive satellite downlink, beamforming techniques at the FSS terminal together with a carrier allocation module proposed in the context of CoRaSat project are reviewed herein. The reader is referred to [32, 31, 33] for more details.

Let  $I_k(m)$  denote the aggregated interference from the whole terrestrial system received at the  $k$ -th FSS terminal for a particular carrier frequency  $f_m$ . These values can be perfectly computed assuming that a geolocation database provides the sufficient information. Subsequently, the SINR values at each FSS terminal and for each carrier frequency are computed. To improve the SINR, we consider the general Linearly Constrained Minimum Variance (LCMV) beamformer proposed by Frost in 1972 [51]. Roughly speaking, the LCMV allows the steered beam to focus onto the satellite direction while imposing multiple linear constraints relative to the FS interference directions. The LCMV is given by,

$$\mathbf{b} = \hat{\mathbf{R}}_y^{-1} \mathbf{C} \left( \mathbf{C}^H \hat{\mathbf{R}}_y^{-1} \mathbf{C} \right)^{-1} \mathbf{g}, \quad (6)$$

where  $\mathbf{g} = \begin{bmatrix} 1 & 0 \end{bmatrix}^T$ ,  $\mathbf{C} = \begin{bmatrix} \mathbf{s}_d & \mathbf{s}_i \end{bmatrix}$  is the constraint matrix with  $\mathbf{s}_d$  and  $\mathbf{s}_i$  being the array response vector towards the satellite and towards the strongest interfering FS station, respectively, and  $\hat{\mathbf{R}}_y$  is used to denote the sample covariance matrix of the received signal. Note that only one FS direction is null-steered due to the limited number of antennas, which is set to 3 throughout this paper. The SINR

values are updated with the corresponding SINR value after beamforming and they are denoted as  $\text{SINR}_{BF}(m, k)$ .

Finally, the  $\text{SINR}_{BF}(m, k)$  values are fed to the carrier allocation module in order to allocate the available spectrum resources. The goal is to design the carrier allocation matrix,  $\mathbf{A}$ , whose elements  $[\mathbf{A}]_{(m,k)}$  work as an indicator function: “1” if  $m$ -th carrier is assigned to the  $k$ -th user and “0” otherwise. According to this notation, the maximization of the cognitive satellite sum-rate can be expressed as [33],

$$\max_{\mathbf{A}} \quad \|\text{vec}(\mathbf{A} \odot \mathbf{R}(\text{SINR}_{BF}))\|_{l_1} \quad \text{s.t.} \quad \sum_{k=1}^K \mathbf{a}_k(m) = 1, \quad (7)$$

where  $\odot$  denotes the Hadamard product,  $\text{vec}(\cdot)$  denotes the vectorization operator,  $\|\cdot\|_{l_1}$  denotes the  $l_1$ -norm and  $\mathbf{R}(\text{SINR})$  denotes the rate matrix with elements  $r(m, k)$ ,  $k = 1, \dots, K$ ,  $m = 1, \dots, M$ , being the DVB-S2X rate [47] associated with the corresponding SINR value. Note that the constraint  $\sum_{k=1}^K \mathbf{a}_k(m) = 1$  in (7) ensures that only one carrier frequency is assigned per user. The optimization problem in (7) can be solved using the efficient Hungarian algorithm [52].

**3.4.2. Scenario C (uplink)** In the uplink scenario, the transmit power and the bandwidth allocated to the satellite terminals has to be controlled such that the aggregated interference caused at the FS system is kept below some acceptable thresholds [53, 54, 33].

In this paper, we review a sub-optimal approach from [33] which ensures to never exceed the prescribed interference threshold. First, the transmit power and the carrier frequencies are jointly optimized. Next, a bandwidth allocation scheme is applied which guarantees protection of the terrestrial FS system while maximizing the satellite total throughput.

The basic idea is to identify the worst FS link per user in terms of interference and divide its amount of tolerable interference among the maximum number of FSS terminal users that share the spectrum with it. Let matrix  $\mathbf{G}(m) \in \mathbb{R}^{K \times L}$  denote the cross-channel link gain from the FSS terminals to the FS stations for a particular carrier frequency  $f_m$  and let  $g_{k,l}(m)$  denote each of its elements, where  $k$  and  $l$  refer to FSS terminal and FS station, respectively. The first step is to identify the FS receiver that gets the highest level of interference from each of the FSS users. This can be done by examination of the highest values of matrix  $\mathbf{G}(m)$  as follows,

$$l_w(m, k) = \max_l [\mathbf{G}(m)]_k, \quad (8)$$

where  $[\mathbf{G}(m)]_k$  denotes the  $k$ -th row of matrix  $\mathbf{G}(m)$  and  $l_w(m, k)$  indicates the index of the worst FS station in terms of interference of user  $k$  operating in carrier  $m$ .

Once the worst FS station is identified, the maximum allowable transmit power per user and per carrier is determined dividing the interference limit of the FS station among the total number of interferers that fit within the FS receiver bandwidth. In other words,

$$I_w(m, k) = I_{\text{thr}, l_w(m, k)} \left( \frac{B^{\text{FS}}}{B^{\text{FSS}}} \right)^{-1}, \quad (9)$$

where  $I_{\text{thr}, l_w(m, k)}$  [W] denote the interference limit of the  $l_w(m, k)$  FS station, and  $B^{\text{FS}}$  and  $B^{\text{FSS}}$  denote the filter bandwidth of the FS station and the FSS terminal, respectively. Consequently, for each  $m$ -th carrier frequency and each  $k$ -th FSS terminal, the power assignment is obtained in such a way that it respects the interference constraint given by,

$$I_w(m, k) \geq p(m, k) \cdot g_{k, l_w(m, k)}(m). \quad (10)$$

The maximum allowable transmit power,  $p_{\text{max}}(m, k)$ , can be obtained from (10) by isolating  $p(m, k)$ . The value of  $p_{\text{max}}(m, k)$  cannot exceed a given maximum and should be high enough to ensure the minimum SINR to close the link. Therefore, the following adjustments are considered,

$$p(m, k) = \max(0, \min(p_{\text{max}}(m, k), P_k^{\text{max}})). \quad (11)$$

Next step is to design the carrier allocation matrix  $\mathbf{A}$  for the uplink. Note that the knowledge of matrix  $\mathbf{A}$  combined with the knowledge of  $\mathbf{p}_k = [p(1, k) \ p(2, k) \ \dots \ p(M, k)]$ ,  $M$  being the total number of frequencies, solves the power allocation problem as the corresponding powers can be computed as  $p_k = \mathbf{a}_k^H \mathbf{p}_k$ , where  $\mathbf{a}_k \in \mathbb{R}^{M \times 1}$  denotes the  $k$ -th column of  $\mathbf{A}$ . Similarly to the downlink case, matrix  $\mathbf{A}$  is obtain by solving the following optimization problem [33],

$$\max_{\mathbf{A}} \quad \|\text{vec}(\mathbf{A} \odot \mathbf{R}(\mathbf{SINR}_{\text{rtt}}))\|_{l_1} \quad \text{s.t.} \quad \sum_{k=1}^K \mathbf{a}_k(m) = 1. \quad (12)$$

Once transmit powers and carriers are assigned, the satellite bandwidth is dynamically allocated to the FSS terminals according to users' rate demands. Let  $R_k$  denote the requested rate by the  $k$ -th FSS terminal. Each rate demand can be mapped to a particular Spectral Efficiency (SE) as follows,  $SE_k = R_k/B_k$ , where  $B_k$  denotes the bandwidth assigned to user  $k$ . Then, the minimum SINR value associated with  $SE_k$  can be extracted from the DVB-S2X standard tables [47]. Therefore, for each rate demand  $R_k$ , we have multiple minimum SINR values depending on the assigned bandwidth. To choose the optimal bandwidth, an ad-hoc algorithm is applied, which obtains the required transmitted power per different bandwidth values to achieve the requested demand. Then, it selects the minimum bandwidth that provides a transmit power below  $P_k^{\text{max}}$  and that satisfies the interference threshold at the terrestrial system.

## 4. RESULTS

### 4.1. Area Analysis

The use of the tools presented in Section 3.1 enables the assessment of the level of interference experienced at a defined FSS terminal position. As background to presenting the results of the database modeling approach some further details are presented here. The information in a database is normally listed on a carrier by carrier basis for a frequency band of interest. All carriers are usually detailed with their frequencies and channel bandwidths. When the database relates to satellite

terminals the database should also contain details on the associated satellite in terms of satellite longitude and the earth stations azimuth and elevation angles. Polarization and antenna gain are also required along with the antenna radiation patterns as defined in ITU Recommendations for use in regulatory work or ETSI standards. In addition, transmission power and equivalent isotropic radiated power (EIRP) may also be included.

A UK BSS database, made available for this study, is used for scenario A and contains 442 carriers from a total of 31 BSS uplink earth stations at 8 physical sites, to 12 different satellites, and is shown in Figure 7. The locations of all these 31 BSS earth stations are marked with an indication of the direction of the beam to the satellite. The number of carriers of each BSS earth station ranges from 1 to 42. The carriers span the range 17.3 GHz to 18.35 GHz. The bandwidths of the carriers that belong to the same BSS earth station are equal, while those belonging to different earth stations might be different and are typically 26 MHz, 33 MHz, 36 MHz or 66 MHz. The EIRP of these earth station antennas ranges in 69 dBW÷84 dBW and all antenna radiation patterns are according to ITU-Recommendation S.465 [39] or S.580 [55].

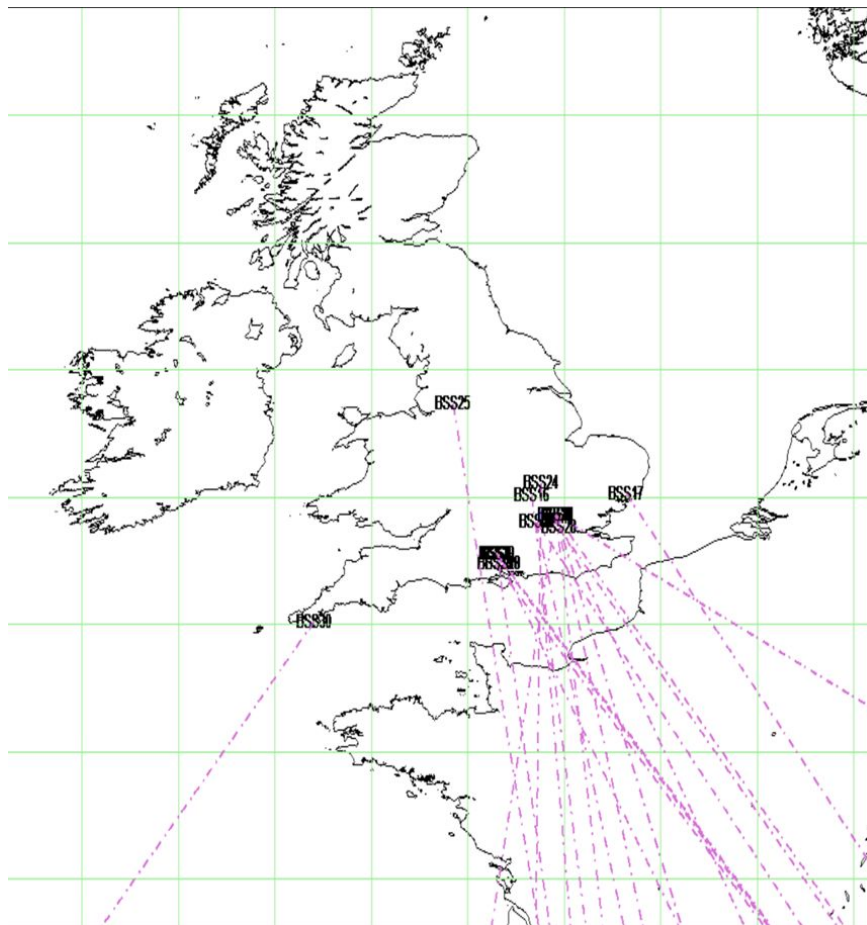


Figure 7. BSS Feeder link sites in the UK.

FS databases at 18 GHz are required for evaluating the scenario B. Again, an FS database was made available to this project (under the UK Freedom of Information Act). The database for the UK FS in the band 17.7 to 19.7 GHz is much larger than that for the UK BSS one and contains 12,712



links with 15,970 carriers recorded in the UK. A French database has also been examined at 18 GHz and is based on the latest ITU-R terrestrial services BR IFIC database [56], which contains 11,548 links with 17,384 carriers recorded. Figure 8 illustrates the FS links in the band 17.7 to 19.7 GHz in the UK and it can be seen that the FS links are much denser than for the BSS. Further databases for Hungary, Poland and Slovenia were obtained and analyzed.

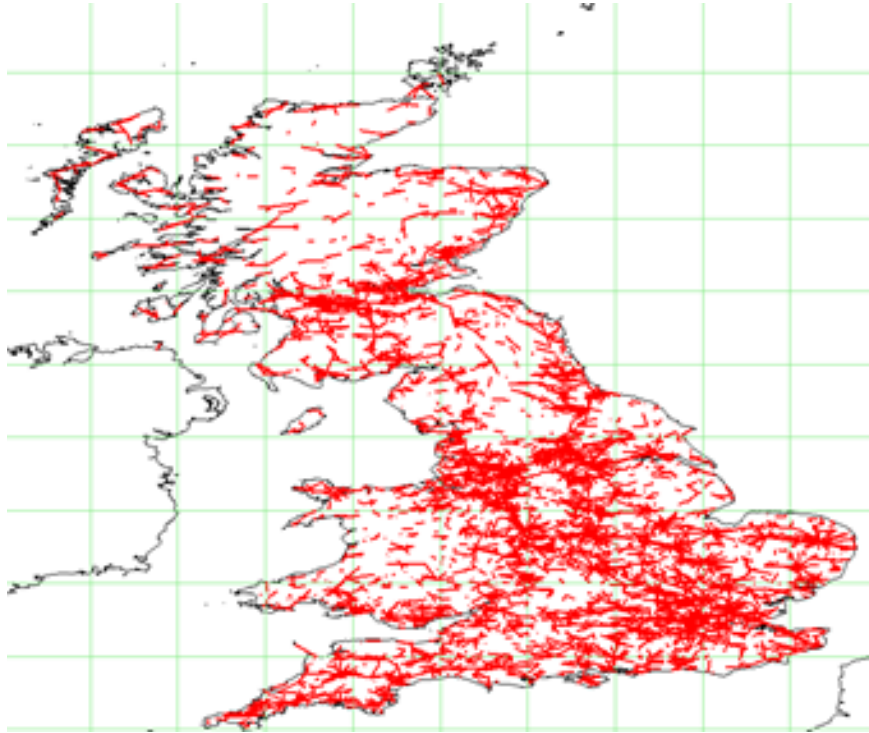


Figure 8. FS links in the UK (18 GHz band).

Figure 9 shows the plots of cognitive zones around a number of BSS Stations under scenario A based on the ITU-R P.452-15 model. Similarly, Figure 10 shows a plot of cognitive zones around a FS Station for the scenario B. For the BSS cognitive zones, the FSS terminal evaluated points to a satellite at 53E longitude and the BSS transmitting terminal points to a satellite at 28.2 degree while for the FS cognitive zone the FSS terminal is pointing to a satellite at 20E longitude and the FS transmitting terminal is pointing at a receive terminal on a bearing of 110 degrees East of True North (ETN).

Scenario B calculations have been performed for analysis of an FSS terminal being located over a fine grid of locations in the UK. The resulting interference levels were then analysed in order to assess the amount of FS spectrum that exceeds the threshold at the FSS sites. The FS bandwidth on a grid over the UK is given in Figure 11.

Calculations have been performed to assess the impact of the FSS antenna pointing to the satellite when the latter varies in the set 53E, 13E, 0E and 34W degrees longitude. As an example, a range of FSS terminal locations from 8W to 2E at a longitude of 51.5N were used to assess the impact. Figure 12 depicts the total bandwidth occupied by FS interferers along the path. From these figures it can be seen that the assumption that the 53E longitude satellite represents the worst case scenario is validated.



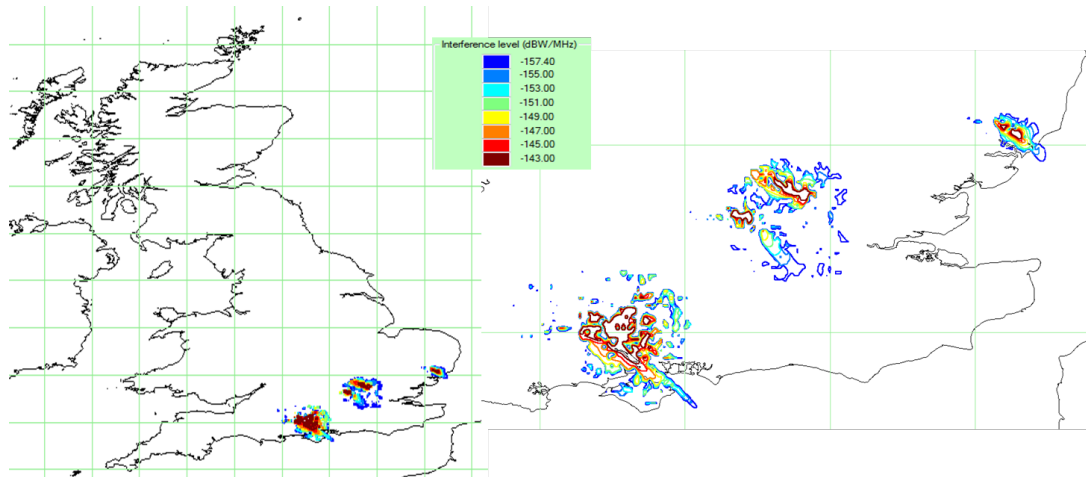


Figure 9. Example Cognitive zones for Scenario A in UK.

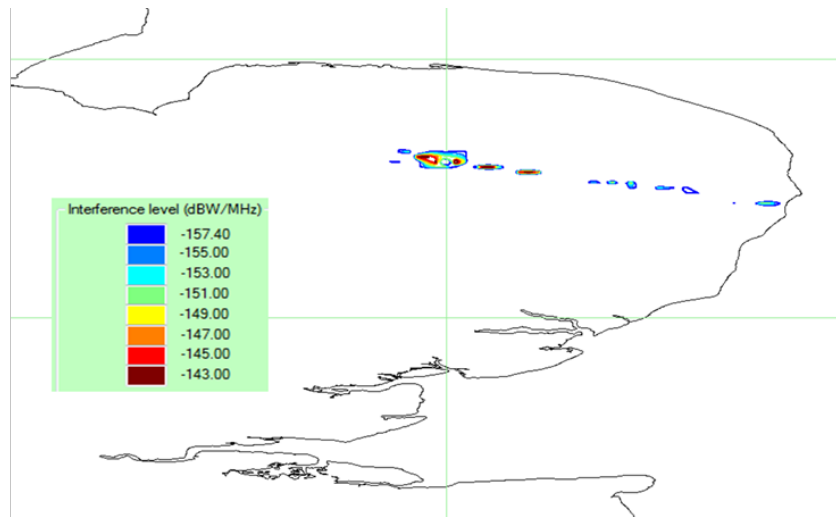


Figure 10. Example Cognitive zones for Scenario B in UK.

Analysis was performed using the databases for the UK, France, Hungary, Poland and Slovenia and the results derived in the form of cumulative distribution functions (CDFs) of the number of FS interfering links that exceed the -154 dBW/MHz threshold at each point, as depicted in Figure 13, as well as the FS bandwidth used over the land masses of each country at that threshold, as depicted in Figure 14. Extracted data is also shown in Table V for ease of understanding.

Table V. CDF of total bandwidth of FS link interference per FSS site (percent of 17.7 - 19.7 GHz)

Percent. of Sites	UK	FRANCE	POLAND	HUNGARY	SLOVENIA
10 percent	7	3	4	2	3
1 percent	23	13	10	14	8
0.1 percent	35	28	20	41	20

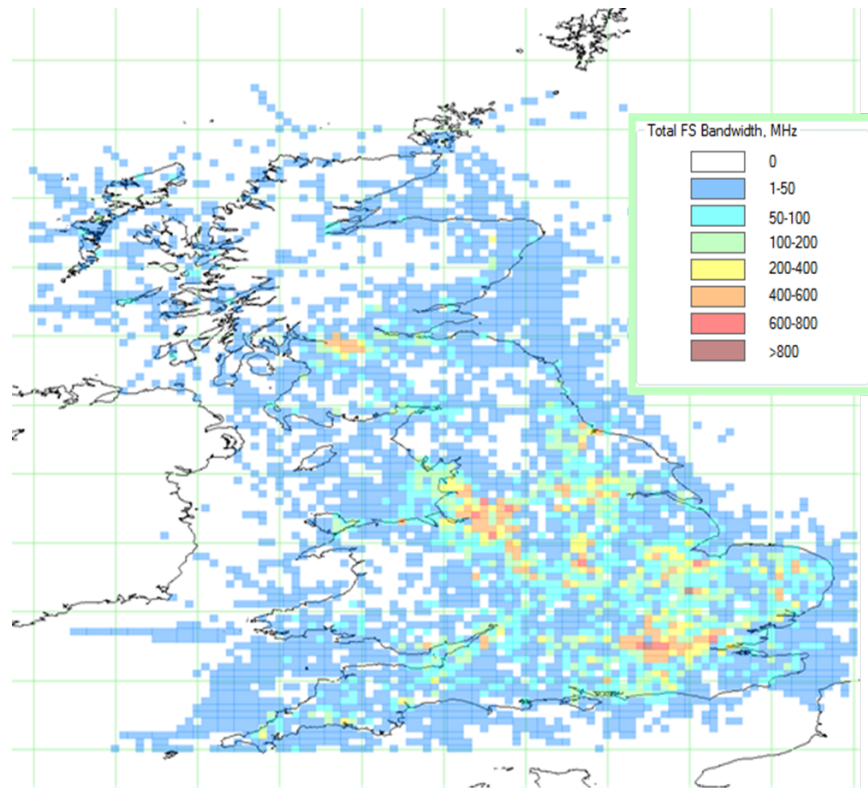


Figure 11. Bandwidth occupied by FS in the UK.

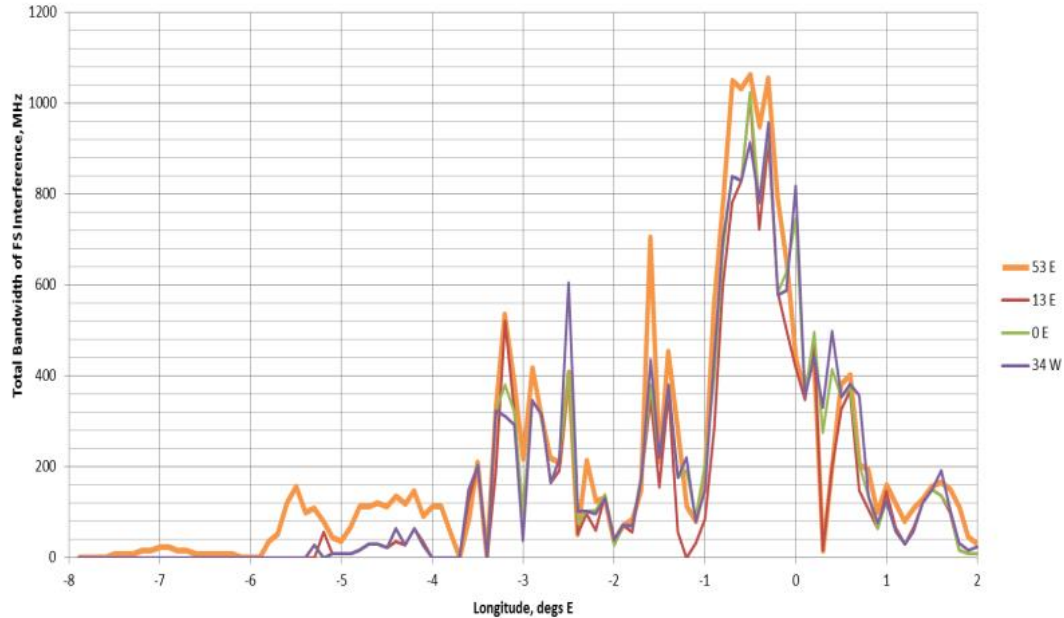


Figure 12. Total Bandwidth occupied by FS interferers for different satellite locations (longitude).

The high number and density of FS links in the UK database makes this the most likely worst case scenario which has been confirmed from the analysis results. Thus if shared spectrum is possible in the UK, then it can be considered to be even more feasible in other countries.

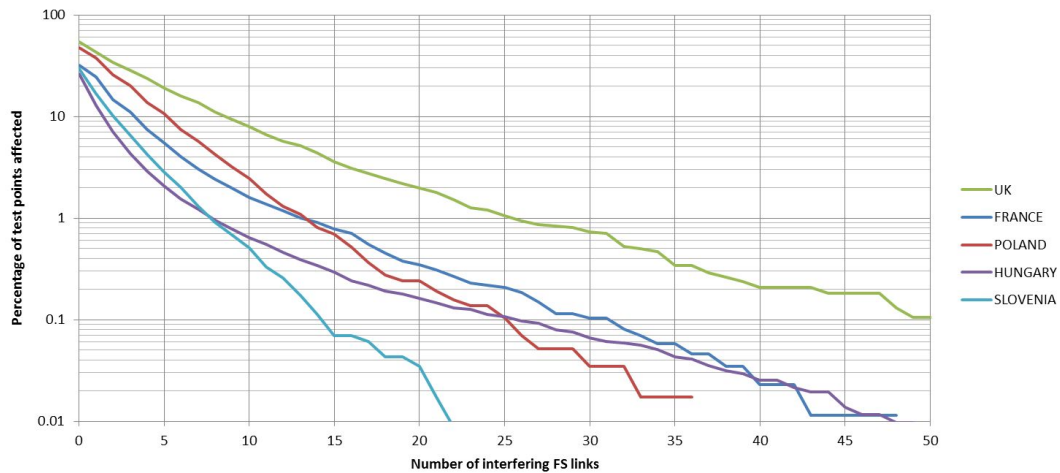


Figure 13. CDF of number of interfering links

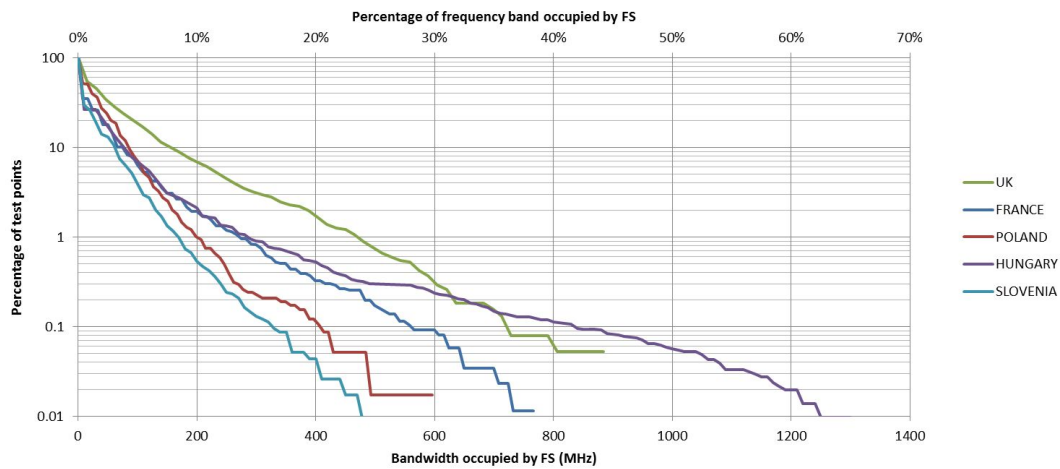


Figure 14. CDF of bandwidth used by FS

#### 4.2. Spectrum Sensing Analysis and Databases

In this section, we discuss the numerical results of the proposed interference estimation technique. While the algorithm assessment has been already discussed in [26, 57], we focus here on its applicability to the proposed scenarios.

**4.2.1. Scenario A** In order to assess the performance of the SNORE based estimation algorithm, a comparison with data representing the ground interference values for a certain cognitive scenario has been made according to the following approach.

The interference levels to be estimated with the SNORE algorithm at a given geographical location has been obtained in [58, 59] by assuming the presence of incumbent systems and by computing the interference level through ITU-R Recommendation P.452-15 [15]. The input parameters to be initialized are related to the terminal antenna that performs SINR estimation; as inputs it is possible to set the FSS terminal coordinates (*latitude*, *longitude*), the longitude of the

FSS satellite  $L_{sat}$  that the terminal points at, the SNR defined as signal to noise ratio  $P_0/N$ , and the number of pilot blocks  $W$ . Thus, the corresponding values estimated by the SNORE estimation block and those used as a reference are compared. These reference interference values are evaluated from the interference model proposed in ITU-R Recommendation P.452-15 [15] used for modelling the interference path losses.

In particular, this approach aimed at understanding how accurate the estimation process is for a fixed terminal antenna in the frequency range to be scanned, and which bands are temporarily/geographically vacant.

To this aim some geographic evaluations have been performed. In particular, the potential geographic reuse factor of a specific carrier frequency as a function of the relative location between interferer sources and the interfered terminal are provided. Table VI lists the parameters used for these simulations. In Fig. 15, the maps describing SINR values obtained from databases and those estimated by a terminal in each point of the area, for different pointing antenna angles, are compared. The results confirm that different pointing angles generate different interference patterns, as expected. Moreover, a correctly estimated large area leads to a better exploitation of geographically available spectrum. The percentages of terminals that have performed the estimation with an error higher than the target,  $\sigma_\epsilon^2|_t/\text{SINR}^2$  equal to 0.1, are 0.39% in Figure 15. Thus, thanks to an accurate estimation of the SINR, the FSS system would be able to avoid high interferences and effectively reuse geographically available spectrum resources.

Table VI. Simulation parameters for geographic assessments

	Parameters
Frequency [GHz]	17.634
SNR [dB]	4
FSS Terminal latitude [°]	from 51.4 to 52.4
FSS Terminal longitude [°]	from -1.0 to 0.2
$L_{sat}$ [degree]	-34E
$W$	10
$B_W$ [MHz]	36
Frame Modulation	QPSK
$N_{pilot}$ [ $\frac{\text{symbol}}{\text{pilot block}}$ ]	36

**4.2.2. Scenario B** In the Scenario B, we have focused on a similar approach while considering also impairments that may occur at the receiver during the estimation process. System reference values taken into account for simulations are reported in Table VII.

The SNORE based technique has also been assessed in the presence of impairments with respect to its applicability in the specific scenario; the three specific impairments cases which have been selected among all the possible for their significance are listed in Table VIII. Both evaluations in frequency domain for a specific earth terminal and in geographic domain considering a wide region covered by the satellite beam pattern are performed by starting from reference results obtained on databases analysis [60].

Geographic assessments are performed to evaluate the SINR estimation process within the beam coverage. Thus, the area from 47N to 48N of latitude and from 19E to 20E of longitude is considered. The SINR values ideally obtained through the use of a database that earth terminals

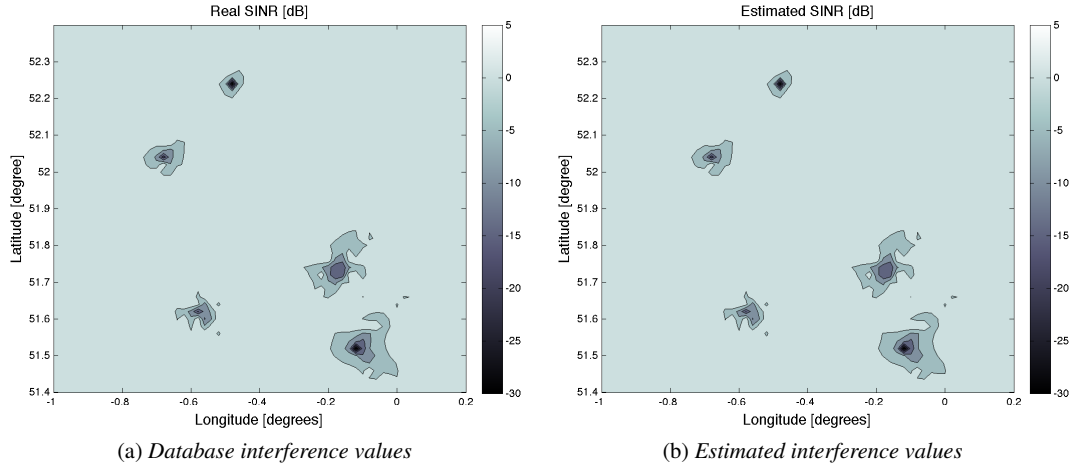
Figure 15. Geographic domain assessments for  $L_{sat} = -34E$ .

Table VII. System Reference Parameters for SNIR based sensing simulations

Parameter Name	Value
Sky Temperature ( $T_{SKY}$ )	15 K
Ground Temperature ( $T_{GROUND}$ )	45 K
Temperature of the Medium ( $T_M$ )	275 K
Downlink Frequency	18.4 - 18.8 GHz
Satellite EIRP ( $EIRP_{SAT}$ )	50 - 70 dBW
Carrier Bandwidth	36 MHz
Terminal Efficiency	0.65
Terminal Antenna Diameter	0.6 meters
Figure of merit ( $G/T$ ) <sub>ES</sub>	34.9 dB/K
Additional ( $G/T$ ) <sub>ES</sub> variation ( $\Delta_2$ )	0 - 2 dB
Antenna gain ( $G_R$ )	50 - 62 dB
Polarization Losses ( $L_{POL}$ )	0 - 0.5 dB
Pointing Losses ( $L_R$ )	0 - 1 dB
Feeder Losses ( $L_{FRX}$ )	0 dB
Terminal Antenna Temperature ( $T_A$ )	78 K
Effective noise temperature ( $T_{eRX}$ )	262 K
Terminal Component Temperature ( $T_F$ )	290 K
Default Temperature ( $T_0$ )	290 K
LNA Noise Factor (NF)	1.4 dB
QPSK Symbols per pilot	36

Table VIII. The selected impairments cases

	Ideal case	Case 1	Case 2	Case 3
Polarization Losses ( $L_{POL}$ ) [dB]	0	0.5	0.5	0.5
Pointing Losses ( $L_R$ ) [dB]	0	1	1	1
Additional ( $G/T$ ) <sub>ES</sub> variation ( $\Delta_2$ ) [dB]	0	2	2	2
Additional atmospheric attenuation ( $A_p$ ) [dB]	0	0	5	10

experience within the coverage, are shown in Fig. 16. It can be noted the presence of a directive

incumbent link and of some incumbent-free regions. Fig. 17 shows the results for the cases listed in Table VIII, for 1 pilot block.

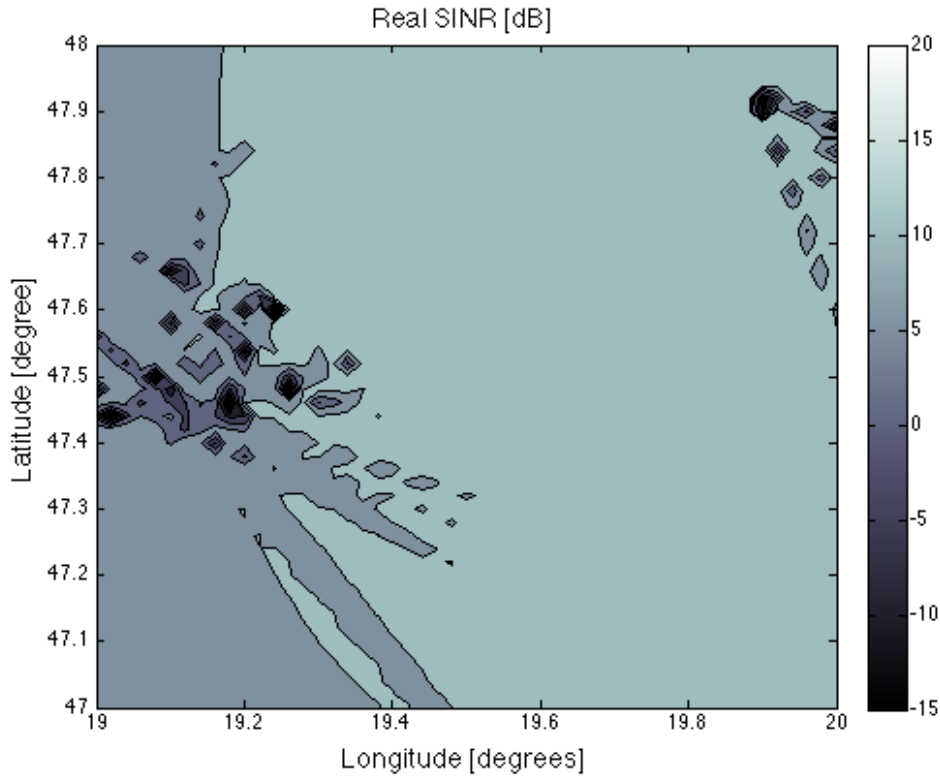


Figure 16. Real SINR values along the selected geographic region

Results obtained from geographic simulations also confirm link budget losses due to presence of impairments and a more reliable estimation due to longer observation periods. Percentages of the SINR values estimated that differ from the real value more than  $\frac{\sigma_{\epsilon|des}^2}{SINR^2} = 0.1$ , where  $\sigma_{\epsilon|des}^2$  is the difference between the real value and the estimated value under uncertainties conditions, are shown in Table IX, where the results with 1 pilot block are also reported. Results show that for both 1 and 10 pilot blocks impairments lead to a degradation of the percentages of points correctly estimated. However, in presence of low impairments losses as for the Ideal case and Case 1, longer estimations provide more reliable estimations whereas in case of higher impairments losses the estimated values do not satisfy the target reliability even in case of longer sensing periods.

Table IX. Geographic assessments results

Case	1 pilot block	10 pilot blocks
Ideal case	0.48%	0.19%
Case 1	0.71%	0.56%
Case 2	2.42%	2.46%
Case 3	3.67%	3.71%

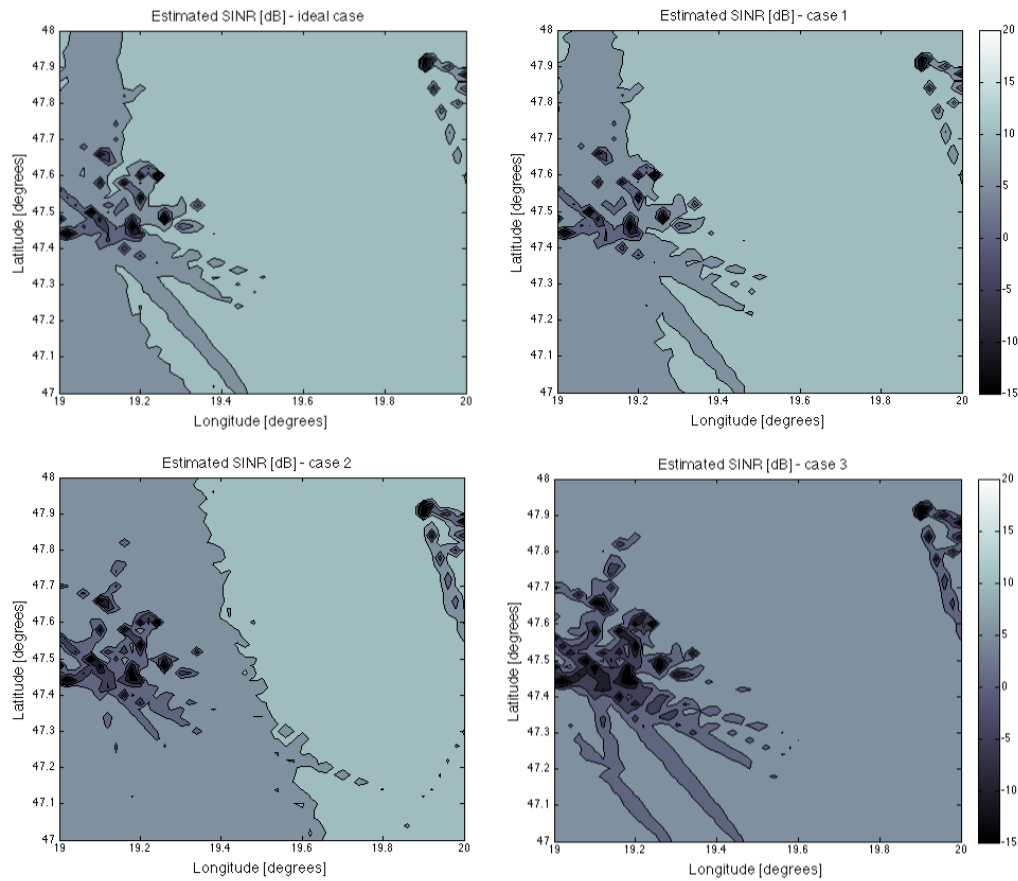


Figure 17. Comparison between estimated values under different impairments conditions

#### 4.3. Capacity Analysis and the use of RA

In this section, we review the capacity analysis obtained for Scenario B (downlink) and C (uplink) considering the proposed cognitive exploitation techniques on an assumed model HTS Satellite. Note that the area analysis presented in Section 4.1 is based on cognitive zone, i.e. the geographical area in which a particular carrier can be used by FSS terminal without applying resource allocation techniques. Here, we go one step further by optimizing the available resources to maximise the capacity. Table X details the databases and the simulation parameters that have been considered to obtain the simulation.

Table X. Summary of the databases and parameters used in the capacity analysis

	Scenario B (downlink)	Scenario C (uplink)
Country evaluated	France	Finland
FS System	ITU-R BRIFIC [56]	Finnish COmmunications Regulatory Authority (FICORA)
$B^{FSS}$	62.4 MHz	7 MHz
Shared band	17.7 – 19.7 GHz (32 carriers)	27.5 – 29.5 GHz (285 carriers)
Exclusive band	19.7 – 20.2 GHz (8 carriers)	29.5 – 30 GHz (71 carriers)
EIRP	65 dBW (Satellite)	50 dBW (FSS terminal)
FSS locations	According to population density obtained from the NASA Socioeconomic Data and Applications Center (SEDAC) [61]	
Terrain altitude	US National Geospatial-Intelligence Agency (NGA) [62]	
Satellite beam pattern	True beam pattern from 13°E EUTELSAT	
Reuse pattern	4 color (freq./pol.)	
Satellite height	35,786 Km	
Gain FSS terminal antenna	42.1 dBi	
Terminal height	15 m	



Essentially, a single country was evaluated for each of the scenarios, namely France for the cognitive satellite downlink and Finland for the uplink counterpart. For each country, the final capacity calculation was obtained after proper weighting of the evaluation carried out for a set of representative beams that fall within the country borders. The representative beams were chosen based on FS link deployment density. The selected beams are depicted in Fig. 18. The performance of the cognitive satellite system was evaluated by averaging over 50 independent FSS terminal geographical distributions. The number of FSS terminals per beam was set to be equal to the number of carriers to be assigned, this is 40 for Scenario B and 356 for Scenario C. The results with beamforming are obtained assuming that each FSS terminal is equipped with 3 LNBS. For more details on the methodology, the reader is referred to [33].

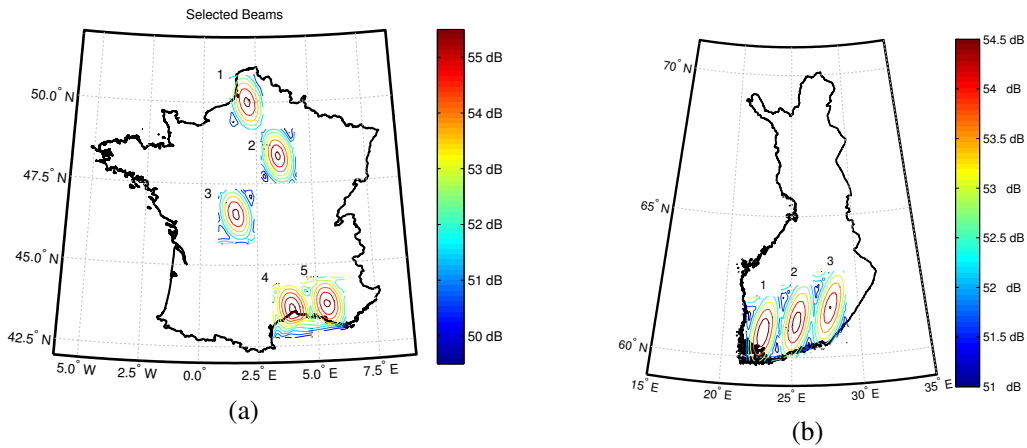


Figure 18. (a) Selected beams for downlink evaluation in France, and (b) Selected beams for uplink evaluation in Finland.

For the capacity analysis, we considered the following cases:

- **Case 1 - Exclusive only:** Only carriers in the exclusive band are considered. This denotes the conventional system without the use of cognitive SatCom.
- **Case 2 - Shared plus exclusive without the presence of any FS system:** Both shared and exclusive band carriers are considered, but in the absence of FS system. This represents the scenario where the additional spectrum is allocated exclusively to FSS system. This case does not exist in practice but is considered useful as a benchmark for comparison purposes.
- **Case 3 - Shared plus exclusive with the presence of FS system:** This depicts the scenario where the FSS system uses carriers in the shared bands as well as the exclusive band and FS interference may be present.

The capacity results are shown in Table XI. The case indicated as “w/o RA” means that a random resource allocation has been carried out, which is worse or as good as the optimal case indicated with “w/ RA”. The use of the beamforming technique is indicated with “BF”. In Table XI we show in parenthesis the % of improvement with respect to the state-of-the-art, i.e. Case 1 w/o RA.

Regarding the capacity analysis for scenario B, as shown in Table XI, clearly, the application of smart carrier allocation does not provide much gain in the exclusive only case. This is mostly



due to the fact that all the available carriers experience similar SINR values. The capacity of the satellite system increases from 686.56 to 3443.74 Mbps when using the 2 GHz of extra spectrum on top of the traditional 500 MHz of the exclusive band. This capacity can be further improved when using the proposed resource allocation techniques. In summary, the average throughput per beam gain through the use of smart carrier allocation is 402.67% over the exclusive only case, which can be further increased with a 3.25% using beamforming technique. In addition, it is worth noting that the use of cognitive exploitation techniques allow the satellite system to achieve similar average capacity as if there were no FS system present in the scene.

Table XI. Per beam average throughput (Mbps)

Scenario	Case 1		Case 2		Case 3		
	w/o RA	w/ RA	w/o RA	w/ RA	w/o RA	w/ RA	w/ RA+BF
Scenario B (downlink)	686.56 (Ref.)	686.84 (0.04%)	3444.97 (401.77%)	3451.16 (402.67%)	3443.74 (401.59%)	3451.13 (402.67%)	3473.46 (405.92%)
Scenario C (uplink)	1108.75 (Ref.)	1108.75 (0%)	5517.64 (397.65%)	5522.87 (398.12%)	5479.32* (394.19%)	5522.87** (398.12%)	

\* Achieved with suboptimal power and carrier allocation but satisfying the interference threshold.

\*\* Achieved with optimal power and carrier allocation satisfying the interference threshold.

Regarding the capacity analysis for scenario C, the nominal interference threshold for an FS receiver was set at -146 dBW/MHz and the maximum power  $P_k^{\max}$  that a satellite terminal can transmit is equal to 7.9 dBW. Results shown in Table XI confirm the additional spectrum together with the resource allocation techniques provide 398.12% improvement over the conventional exclusive band case. However, the gain achieved with a sub-optimal allocation of resources is slightly lower than the one achieved with the optimal one. This is because the deployment of FS links in the 28 GHz band is rather sparse in Finland and very few satellite terminals are forced to reduce their transmit power to not violate the FS interference threshold. In view of this results, it can be concluded that, using the smart resource allocation, we can achieve the same throughput as if there were no FS system, while ensuring protection to the FS.

Regarding the bandwidth allocation technique for scenario C, the rate demands per user are randomly generated at each realization. It is assumed that these demands are not greater than the maximum that can be achieved with 7 MHz bandwidth. Table XII shows the obtained results. In Table XII, the values in parenthesis represent the mean values achieved considering that the satellite terminals operate on a fixed 7 MHz bandwidth, i.e., without considering bandwidth allocation.

It can be observed that the bandwidth and the transmitted power have been reduced as a consequence of reduction of the mean user demand, which is half of the maximum demand that was assigned when considering the whole 2.5 GHz bandwidth. In conclusion, the bandwidth allocation scheme satisfies the user rate demands and prevents an unnecessary waste of resources by maximizing the effectiveness of their utilization.

Table XII. Bandwidth allocation results

	Rate [Mbps]	Bandwidth [MHz]	Power [dBW]
Mean value	7.5065 (15.0903)	3.4463 (7)	3.2276 (7.888)

#### 4.4. Earth Stations on Mobile Platforms (ESOMP) analysis

We have also addressed potential Ka-band operation of ESOMPs in the shared bands. The ESOMPs cases considered are as follows:

- Case 1: Aircraft-mounted ESOMP with downlink in the band 17.7-19.7 GHz and uplink in the band 27.5 to 30 GHz.
- Case 2: Ship-mounted ESOMP with downlink in the band 17.7-19.7 GHz and uplink in the band 27.5 to 30 GHz.

For Case 1 the situation is quite complex. The very directive nature of the FS antennas and the airborne antenna contribute very significantly to the level of interference and the number of significant interfering links, which vary quite rapidly as the aircraft travels along its flight path. Scenarios A, B and C can be considered for such cases where the FSS terminal is the ESOMPs terminal.

Analysis of Scenarios A and B for this case indicates that the above mentioned antenna effects will help reduce the cumulative interference levels to values that can be managed by appropriate mitigation techniques. An example of such analysis is given below. For both cases 1 and 2, for Scenario C we have limited our considerations to the case where in Europe the availability of the two High Density FSS (HDFSS) bands may be adequate for such systems and interference mitigation is not required. However, in other regions of the world this may not necessarily be the case. Work elsewhere has been addressing this matter in considerable detail [63, 64].

**Case 1 Aeronautical ESOMP.** The methodology adopted earlier using ITU-R P.452-15 [15] can be extended to an aeronautical case by applying a number of critical modifications. These are:

1. Increase the height above mean sea level of the victim receiver so that it corresponds to the altitude of the aircraft;
2. Find the range from the FS transmitter to the aircraft for use in the calculations;
3. Find the azimuth and elevation angles of the aircraft as viewed from the FS transmitter;
4. Find the azimuth and elevation angles of the FS transmitter as viewed from the aircraft;
5. Using the above, determine the off-axis angle and thus gain of the FS transmitter antenna;
6. Using the above, determine the off-axis angle and thus gain of the aircraft receiving antenna;
7. Adopt the more complex ITU-R P.676-10 annex 1 model which is applicable to low elevation angles for calculating the gaseous losses;
8. Include the effect of aircraft fuselage attenuation;
9. Adjust the parameters to take account of the fact that the aircraft receive antenna diameter is 0.6 metres.

These modifications have been undertaken and wherever possible validated to be correct. Thanks to an example, we have performed calculations for an airborne ESOMP flying along the *Aero Path* line indicated in Figure 19 at two different altitudes. The first altitude is 3.81 km (12,500 ft) and the second is for 11.88 km (39,000 ft), which is the average of the maximum altitude capability of known commercial airliners. The figure has a background that is indicative of the general interference level in terms of bandwidth used by the FS but is indicative rather than being

specific to ESOMPs. The flight path is therefore over the more dense interference regions of the UK and typical of paths near Heathrow Airport. Detailed airborne ESOMP results are presented in Figure 20 for the 3.81 km altitude case.

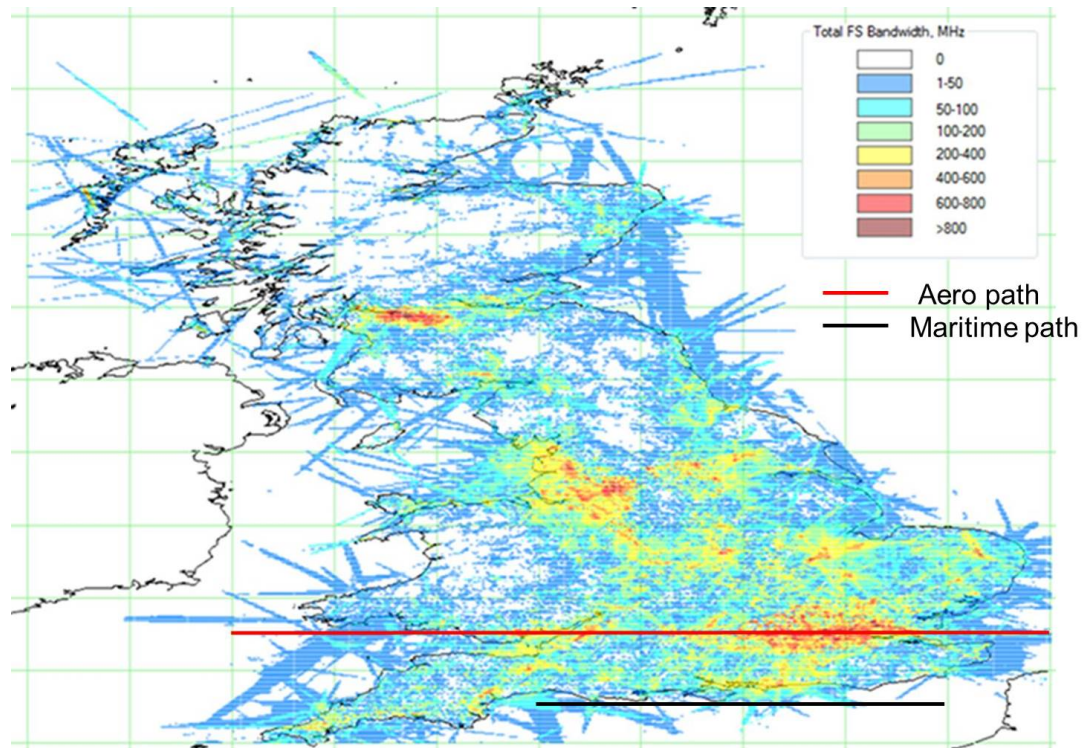


Figure 19. Example Aeronautical and Maritime ESOMP paths.

**Case 2 Maritime ESOMP.** For case 2, when the ESOMP is maritime in nature, Scenarios A and B are simply extended to areas in the sea. In the case of Scenario B, with the ESOMPS ship operating in the 17.7 to 19.7 GHz band, example results are given for a ship sailing along the English Channel as depicted *Maritime Path* in Figure 19 which also presents the indicative interference field for total FS interfering bandwidth for a threshold of -154.5 dBW/MHz at any given point. The path of interest is shown in red and represents a journey of length 284 km.

This example assumes that the ship is sailing in the interested path on the sea along the English Channel and that there are UK based FS microwave stations on the land that may cause interference to the ship-borne ESOMP. Each FS link has its own frequency, bandwidth and the value of interference levels at each particular test point. The shipborne terminal is assumed to be pointing to a satellite located at 13E longitude with the ship receiving signals from the satellite. Antenna patterns, full terrain based propagation models and path losses were all taken into account for this calculation.

The red line, associated with the right hand scale, in Figure 21 (also on Figure 20) represents the percentage of the 2 GHz of available bandwidth that interference from the FS exceeds the given interference threshold along the example path. It should be noted that such total bandwidth may be similar at different locations but be comprised of several carriers at quite different frequencies. The presentation format is the same as that used for the Aeronautical ESOMP.

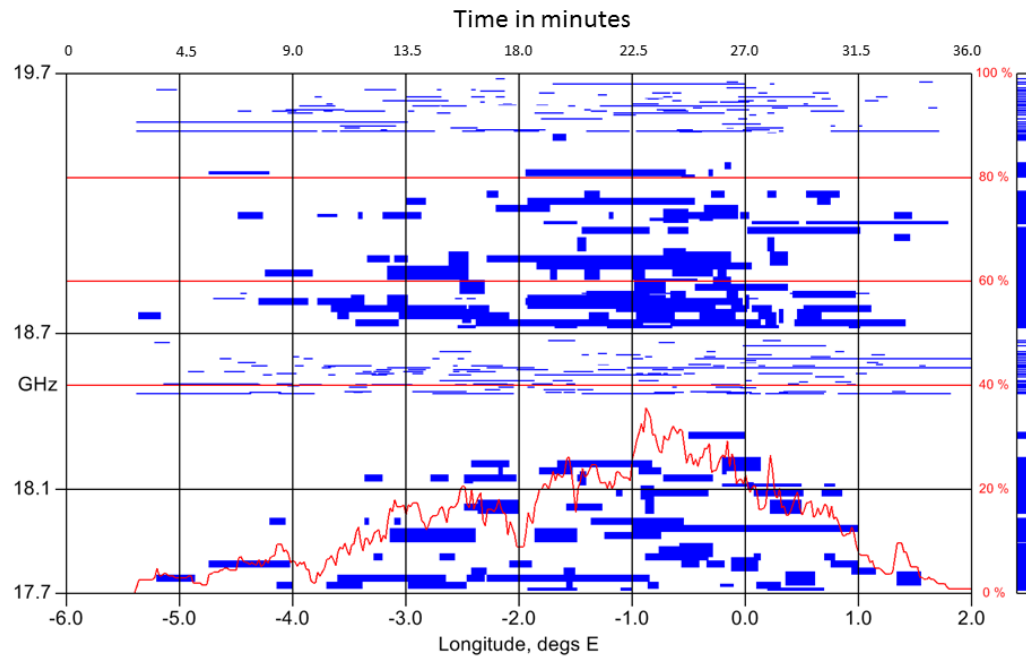


Figure 20. Example Aeronautical ESOMP results.

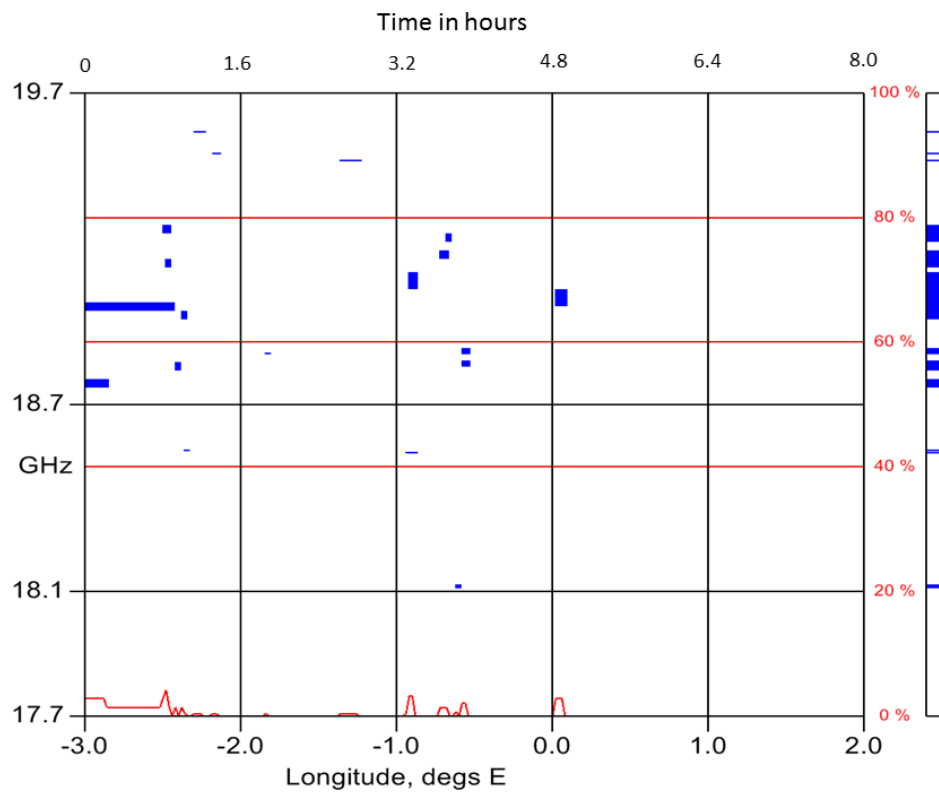


Figure 21. Example Maritime ESOMP results.

It can be seen that significant parts of the 17.7 to 19.7 GHz band are available for use with ESOMPs when the only mitigation approach required is spectrum management within the satellite resource allocation algorithms. The dynamic nature of the required interference driven resource management mechanism is not as fast or critical in the maritime case compared to the aeronautical one due to the lower speed of movement of the ESOMP. The elapsed time from the start of the ESOMP journey is also depicted in Figure 20 and Figure 21.

**ESOMP Summary** Example results for both shipborne and airborne operations have been presented indicating that with appropriate use of cognitive counter measures (especially interference aware radio resource management) there is adequate bandwidth available for mitigating the FS interference. Due to the movement of the terminal of interest causing a time variant element to the interference conditions the interference driven resource management mechanisms need to be much more dynamic than that required for the previously reported FSS cases.

## 5. CONCLUSIONS

Satellite Communications (SatCom) are a key technology in achieving the challenging objective set forth in the Digital Agenda for Europe to provide high-speed broadband access to everyone by 2020. The CoRaSat (COgnitive RADio for SATellite communications) project envisaged a flexible and smart satellite system able to exploit unused or underused frequency resources assigned to other services on a primary or secondary basis. The objective was to maximise resource utilization and to open up novel business perspectives with lower transmission costs, and Cognitive Radio (CR) techniques are considered the most promising solution. To this aim, cognitive approaches and techniques have been investigated, developed, and demonstrated in specific scenarios that are relevant to SatCom. While CR techniques already proved their potential in terrestrial networks, their application in a satellite context is still in its infancy. The CoRaSat project is, thus, the first initiative providing a systematic analysis of CR techniques to SatCom and the related proof-of-concept implementation and demonstration. In this paper the focus is on the description of the main spectrum awareness and exploitation techniques that has been developed for the selected scenarios. To this aim, we have shown that the specific scenarios addressed required the development of original techniques in order to cope with the system requirements. The numerical assessment has shown that the proposed techniques allows a viable spectrum sharing between terrestrial and satellite communications.

We have shown that a database driven modeling approach provides a high degree of confidence that, from both an area analysis and overall system capacity basis, there is adequate means to highly exploit the shared frequency bands. In particular, We have explored the availability of the 2 GHz of spectrum between 17.7 and 19.7 GHz (downlink) and the results have shown that the number of actual interfering FS links are limited due to terrain diffraction effects so that at a particular location substantial parts of the 17.7 to 19.7 GHz are available for FSS use, but not the same frequencies at all locations. This indicates that a database interfaced with a resource allocation scheme could give good access to the increased spectrum.

Moreover an ESOMP analysis has also been carried out showing that the proposed techniques can be used under certain conditions. Our studies indicate that the interference is not too limiting for airborne and maritime ESOMPs operations in terms of interference from FS links into ESOMPs but a more dynamic interference aware resource management system will be required.

With respect to the spectrum sensing we showed that the proposed joint estimation and detection technique allows to increase the performance of the system. In particular in Scenario A, where the incumbents are the BSS feeder links, the proposed approach allows to have a reduced misdetection probability (about 0.39%), while in the Scenario B, where the incumbents are the FS links, the misdetection probabilities range from 0.56% to 3.71% depending on the number of pilot block, also considering transmission impairments.

With respect to the spectrum exploitation techniques, we showed that the smart resource allocation provides significant capacity gains to the cognitive FSS system. For the satellite downlink, the average capacity per beam gain obtained with the proposed RA techniques is 405% over the conventional case, where only exclusive carriers are assigned. For the satellite uplink, the gain achieved by optimally assigning carriers and transmit power is similar to that achieved in the downlink. In addition, the proposed bandwidth allocation makes the most efficient use of the available bandwidth. It is worth to emphasize that, in all cases, the cognitive satellite system is guaranteed to never cause harmful interference to the incumbent FS system."

#### REFERENCES

1. European Commission. A digital agenda for Europe. COM(2010)245 2010. URL <http://eur-lex.europa.eu/legal-content/EN/TXT/?uri=celex:52010DC0245>.
2. Liolis K, Schlueter G, Krause J, Zimmer F, Combelles L, Grotz J, Chatzinotas S, Evans B, Guidotti A, Tarchi D, et al.. Cognitive radio scenarios for satellite communications: The CoRaSat approach. *2013 Future Network and Mobile Summit (FutureNetworkSummit)*, Lisbon, Portugal, 2013.
3. EU FP7 Project CoRaSat (COgnitive RAdio for SATellite Communications) Jun 2016. URL <http://www.ict-corasat.eu/>.
4. Kandeepan S, De Nardis L, Di Benedetto MG, Guidotti A, Corazza GE. Cognitive satellite terrestrial radios. *2010 IEEE Global Telecommunications Conference (GLOBECOM 2010)*, Miami, FL, USA, 2010; 1–6, doi: 10.1109/GLOCOM.2010.5683428.
5. BATS project. URL <http://www.batsproject.eu/>.
6. Fenech H, Lance E, Tomatis A, Kalama M. KA-SAT and the way forward. *Proc. of 2011 Ka and Broadband Communications, Navigation and Earth Observation Conference*, Palermo, Italy, 2011.
7. Viasat-1 launch. URL <https://www.viasat.com/viasat-1-launch>.
8. Thompson P, Evans B, Castenet L, Bousquet M, Mathiopoulos T. Concepts and technologies for a terabit/s satellite. *Proc. of SPACOMM 2011 The Third International Conference on Advances in Satellite and Space Communications*, Budapest, Hungary, 2011; 12–19.
9. Kyrgiazos A, Evans B, Thompson P, Mathiopoulos PT, Papaharalabos S. A terabit/second satellite system for European broadband access: a feasibility study. *International Journal of Satellite Communications and Networking* Mar 2014; **32**(2):63–92, doi:10.1002/sat.1067.
10. CEPT.ORG. URL <http://www.cept.org/>.
11. Maleki S, Chatzinotas S, Evans B, Liolis K, Grotz J, Vanelli-Coralli A, Chuberre N. Cognitive spectrum utilization in Ka band multibeam satellite communications. *IEEE Communication Magazine* Mar 2015; **53**(3):24–29, doi: 10.1109/MCOM.2015.7060478.
12. Electromagnetic compatibility and radio spectrum matters (ERM); System reference document (SRdoc); Cognitive radio techniques for satellite communications operating in Ka band. *TR 103 263*, ETSI Jul 2014.
13. Tarchi D, Guidotti A, Icolari V, Vanelli-Coralli A, Sharma S, Chatzinotas S, Maleki S, Evans B, Thompson P, Tang W, et al.. Technical challenges for cognitive radio application in satellite communications. *2014 9th International*



- Conference on Cognitive Radio Oriented Wireless Networks and Communications (CROWNCOM)*, Oulu, Finland, 2014, doi:10.4108/icst.crowncom.2014.255727.
14. Tv white spaces. URL <http://www.ict-crsi.eu/index.php/standardization-streams/tv-white-spaces>.
  15. Prediction procedure for the evaluation of interference between stations on the surface of the Earth at frequencies above about 0.1 GHz. *Rec. P.452-15*, ITU-R Sep 2013.
  16. Methods for the determination of the coordination area around an earth station in frequency bands between 100 MHz and 105 GHz. *ITU Radio Regulations*, vol. 2. chap. 7, ITU, 2012; 135–230.
  17. System parameters and considerations in the development of criteria for sharing or compatibility between digital fixed wireless systems in the fixed service and systems in other services and other sources of interference. *Rec. F.758-5*, ITU-R Mar 2012.
  18. Haykin S, Thomson D, Reed J. Spectrum sensing for cognitive radio. *Proceedings of the IEEE* May 2009; **97**(5):849–877, doi:10.1109/JPROC.2009.2015711.
  19. Yucek T, Arslan H. A survey of spectrum sensing algorithms for cognitive radio applications. *IEEE Communications Surveys and Tutorials* First Quarter 2009; **11**(1):116–130, doi:10.1109/SURV.2009.090109.
  20. Goldsmith A, Jafar S, Maric I, Srinivasa S. Breaking spectrum gridlock with cognitive radios: An information theoretic perspective. *Proceedings of the IEEE* May 2009; **97**(5):894–914, doi:10.1109/JPROC.2009.2015717.
  21. Urkowitz H. Energy detection of unknown deterministic signals. *Proceedings of the IEEE* April 1967; **55**(4):523–531, doi:10.1109/PROC.1967.5573.
  22. Gardner WA, Napolitano A, Paura L. Cyclostationarity: Half a century of research. *Signal Processing* April 2006; **86**(4):639–697, doi:10.1016/j.sigpro.2005.06.016.
  23. Cabric D, Mishra SM, Brodersen RW. Implementation issues in spectrum sensing for cognitive radios. *Conf. Record of the 38th Asilomar Conference on Signals, Systems and Computers*, Pacific Grove, CA, USA, 2004; 772–776.
  24. Cioni S, Corazza G, Bousquet M. An analytical characterization of maximum likelihood signal-to-noise ratio estimation. *Proc. of 2nd International Symposium on Wireless Communication Systems*, Siena, Italy, 2005; 827–830, doi:10.1109/ISWCS.2005.1547825.
  25. Cioni S, De Gaudenzi R, Rinaldo R. Channel estimation and physical layer adaptation techniques for satellite networks exploiting adaptive coding and modulation. *Int. J. Satell. Commun. Network.* Mar 2008; **26**:157–188, doi:10.1002/sat.901.
  26. Icolari V, Guidotti A, Tarchi D, Vanelli-Coralli A. An interference estimation technique for satellite cognitive radio systems. *2015 IEEE International Conference on Communications (ICC)*, London, UK, 2015; 892–897, doi:10.1109/ICC.2015.7248435.
  27. Jorswieck E, Mochaourab R. Beamforming in underlay cognitive radio: Null-shaping constraints and greedy user selection. *2010 Proceedings of the Fifth International Conference on Cognitive Radio Oriented Wireless Networks & Communications (CROWNCOM)*, Cannes, France, 2010.
  28. Islam H, Liang Y, Hoang A. Joint power control and beamforming for cognitive radio networks. *IEEE Trans. on Wireless Communications* Jul 2008; **7**(7):2415–2419.
  29. Sharma S, Chatzinotas S, Ottersten B. Transmit beamforming for spectral coexistence of satellite and terrestrial networks. *2013 8th International Conference on Cognitive Radio Oriented Wireless Networks (CROWNCOM)*, Washington, DC, USA, 2013.
  30. Sharma SK, Chatzinotas S, Ottersten B. Spatial filtering for underlay cognitive satcoms. *Personal Satellite Services: 5th International ICST Conference, PSATS 2013, Toulouse, France, June 27-28, 2013, Revised Selected Papers*, Dhaou R, Beylot AL, Montpetit MJ, Lucani D, Mucchi L (eds.). Springer International Publishing, 2013; 186–198, doi:10.1007/978-3-319-02762-3\_17.
  31. Sharma S, Lagunas E, Maleki S, Chatzinotas S, Grotz J, Krause J, Ottersten B. Resource allocation for cognitive satellite communications in Ka-band (17.7-19.7 GHz). *2015 IEEE International Conference on Communication Workshop (ICCW)*, London, UK, 2015.
  32. Sharma S, Maleki S, Chatzinotas S, Grotz J, Krause J, Ottersten B. Joint carrier allocation and beamforming for cognitive satcoms in Ka-band (17.3-18.1 GHz). *2015 IEEE International Conference on Communication (ICC)*, London, UK, 2015.
  33. Lagunas E, Sharma S, Maleki S, Chatzinotas S, Ottersten B. Resource allocation for cognitive satellite communications with incumbent terrestrial networks. *IEEE Trans. Cognitive Commun. and Networking* Sep 2015; **1**(3):305–317.
  34. Grotz J, Ottersten B, Krause J. Signal detection and synchronization for interference overloaded satellite broadcast reception. *IEEE Trans. on Wireless Communications* Oct 2010; **9**(10):3052–3063.
  35. Le L, Hossain E. Resource allocation for spectrum underlay in cognitive radio networks. *IEEE Trans. on Wireless Communications* Dec 2008; **7**(12):5306–5315.

36. Zhang R, Liang Y, Cui S. Dynamic resource allocation in cognitive radio networks. *IEEE Signal Processing Magazine* May 2010; **27**(3):102–114.
37. Han Z, Ray Liu K. *Resource Allocation for Wireless Network*. Cambridge University Press: Cambridge, UK, 2008.
38. Vassaki S, Poulakis M, Panagopoulos A, Constantinou P. Power allocation in cognitive satellite terrestrial networks with QoS constraints. *IEEE Communications Letters* Jul 2013; **17**(7):1344–1347.
39. Reference radiation pattern for earth station antennas in the fixed-satellite service for use in coordination and interference assessment in the frequency range from 2 to 31 GHz. *Rec. S.465-6*, ITU-R Jan 2010.
40. ITU-R Study Group 3 (SG3). URL <http://www.itu.int/en/ITU-R/study-groups/rsg3/Pages/default.aspx>.
41. ITU Digitized World Map (IDWM) and Subroutine Library. URL <https://www.itu.int/pub/R-SOFT-IDWM>.
42. Shuttle radar topographic mission (SRTM) 90m digital elevation data. URL <http://srtm.csi.cgiar.org/>.
43. World geodetic system 84. URL <https://www.nga.mil/ProductsServices/GeodesyandGeophysics/Pages/WorldGeodeticSystem.aspx>.
44. GSHHG - a global self-consistent, hierarchical, high-resolution geography database. URL <http://www.ngdc.noaa.gov/mgg/shorelines/gshhs.html>.
45. Technical coordination methods for fixed-satellite networks. *Rec. S.740-0*, ITU-R Mar 1992.
46. Digital Video Broadcasting (DVB); Second generation framing structure, channel coding and modulation systems for Broadcasting, Interactive Services, News Gathering and other broadband satellite applications (DVB-S2). *European Standard EN 302 307*, ETSI Mar 2013.
47. Digital Video Broadcasting (DVB); Second generation framing structure, channel coding and modulation systems for Broadcasting, Interactive Services, News Gathering and other broadband satellite applications Part II: S2-Extensions (DVB-S2X). *European Standard EN 302 307 - 2*, ETSI Mar 2014.
48. Digital Video Broadcasting (DVB); Implementation guidelines for the second generation system for Broadcasting, Interactive Services, News Gathering and other broadband satellite applications; Part II: S2 Extensions (DVB-S2X). *European Standard DVB Document A171-2* Mar 2015.
49. Maral G, Bousquet M, Sun Z (eds.). *Satellite Communications Systems: Systems, Techniques and Technology*. 5th edn., Wiley, 2009.
50. Maleki S, Chatzinotas S, Krause J, Liolis K, Ottersten B. Cognitive Zone for Broadband Satellite Communication in 17.3–17.7 GHz Band. *IEEE Wireless Communication Letters* Jun 2015; **4**(3):305–308.
51. Frost O. An algorithm for linearly constrained adaptive array processing. *Proceedings of the IEEE* Aug 1972; **60**(8):926–935.
52. Kuhn H. The Hungarian Method for the Assignment Problem. *Naval Research Logistics Quarterly* 1955; **2**:83–97.
53. Lagunas E, Sharma SK, Maleki S, Chatzinotas S, Grotz J, Krause J, Ottersten B. Resource allocation for cognitive satellite uplink and fixed-service terrestrial coexistence in ka-band. *Cognitive Radio Oriented Wireless Networks: 10th International Conference, CROWNCOM 2015, Doha, Qatar, April 21-23, 2015, Revised Selected Papers*, Weichold M, Hamdi M, Shakir ZM, Abdallah M, Karagiannidis KG, Ismail M (eds.). Springer International Publishing, 2015; 487–498, doi:10.1007/978-3-319-24540-9\_40.
54. Lagunas E, Sharma S, Maleki S, Chatzinotas S, Ottersten B. Power control for satellite uplink and terrestrial fixed-service co-existence in Ka-band. *IEEE Vehicular Technology Conference (VTC-Fall)*, Boston, MA, USA, 2015.
55. Radiation diagrams for use as design objectives for antennas of earth stations operating with geostationary satellites. *Rec. S.580-6*, ITU-R Jan 2004.
56. BR IFIC for Terrestrial Services. URL <http://www.itu.int/en/ITU-R/terrestrial/brific>.
57. Tarchi D, Icolari VR, Grotz J, Vanelli-Coralli A, Guidotti A. On the feasibility of interference estimation techniques in cognitive satellite environments with impairments. *Wireless and Satellite Systems: 7th International Conference, WiSATS 2015, Bradford, UK, July 6-7, 2015. Revised Selected Papers*, Pillai P, Hu FY, Otung I, Giambene G (eds.). Springer International Publishing, 2015; 133–146, doi:10.1007/978-3-319-25479-1\_10.
58. Performance evaluation of existing cognitive techniques in satellite context. *Del. D3.2*, EU FP7 Project CoRaSat 2014.
59. Adaptation and design of cognitive techniques for satellite communications. *Del. D3.3*, EU FP7 Project CoRaSat 2014.
60. Thompson P, Evans B. Analysis of interference between terrestrial and satellite systems in the band 17.7–19.7 GHz. *Proc. of 2015 IEEE International Conference on Communications Workshops (ICCW)*, London, UK, 2015.
61. NASA. Socioeconomic Data and Applications Center (SEDAC). <http://sedac.ciesin.columbia.edu>. [Online; accessed 30-Apr-2015].
62. NGA. Terrain Data - US National Geospatial-Intelligence Agency. URL [http://geoengine.nga.mil/muse-cgi-bin/rast\\_roam.cgi](http://geoengine.nga.mil/muse-cgi-bin/rast_roam.cgi), [Online; accessed Feb-2015].



63. The use of earth stations on mobile platforms operating with GSO satellite networks in the frequency ranges 17.3-20.2 GHz and 27.5-30.0 GHz. *ECC Report 184*, CEPT Feb 2013.
64. The harmonised use, free circulation and exemption from individual licensing of earth stations on mobile platforms (ESOMPs) within the frequency bands 17.3-20.2 GHz and 27.5-30.0 GHz. *ECC Decision 13(01)*, CEPT Mar 2013.